Optimal scheduling of an active distribution system considering distributed energy resources, demand response aggregators and electrical energy storage

Hamid Zakernezhad [a], Mehrdad Setayesh Nazar [a], Miadreza Shafie-khah [b], João P.S. Catalão [c,*]

[a] *Shahid Beheshti University, Tehran, Iran*
[b] *School of Technology and Innovations, University of Vaasa, 65200 Vaasa, Finland*
[c] *Faculty of Engineering of the University of Porto and INESC TEC, 4200-465 Porto, Portugal*

HIGHLIGHTS

- This paper presents a framework for the optimal scheduling of an active distribution system.
- The distribution system utilizes multiple distributed energy resources.
- Electric vehicle parking lot aggregators and demand response aggregators are considered.
- Different case studies were carried out to assess the effectiveness of the algorithm.

ARTICLE INFO

ABSTRACT

This paper presents a two-level optimization model for the optimal scheduling of an active distribution system in day-ahead and real-time market horizons. The distribution system operator transacts energy and ancillary services with the electricity market, plug-in hybrid electric vehicle parking lot aggregators, and demand response aggregators. Further, the active distribution system can utilize a switching procedure for its zonal tie-line switches to mitigate the effects of contingencies. The main contribution of this paper is that the proposed framework simultaneously models the arbitrage strategy of the active distribution system, electric vehicle parking lot aggregators, and demand response aggregators in the day-ahead and real-time markets. This paper's solution methodology is another contribution that utilizes robust and lexicographic ordering optimization methods. At the first stage of the first level, the optimal bidding strategies of plug-in hybrid electric vehicle parking lot aggregators and demand response aggregators are explored. Then, at the second stage of the first level, the day-ahead optimization process finds the optimal scheduling of distributed energy resources and switching of electrical switches. Finally, at the second level, the real-time optimization problem optimizes the scheduling of system resources. Different case studies were carried out to assess the effectiveness of the algorithm. The proposed algorithm increases the system's day-ahead and real-time revenues by about 52.09% and 47.04% concerning the case without the proposed method, respectively.

1. Introduction

The increasing utilization of Distributed Energy Resources (DERs) provides more control variables for distribution system operators. An Active Distribution System (ADS) can utilize PhotoVoltaic (PV) systems, Wind Turbines (WTs), Demand Side Response (DRP) alternatives, Electrical energy Storage System (ESS) systems, and gas-fueled Distributed Generation (DG) facilities to supply its customers and deliver energy and ancillary services to the wholesale electricity market [1]. Further, the ADS can transact energy and ancillary services with the Demand Response Aggregators (DRAs) and plug-in hybrid Electric Vehicle Parking Lot Aggregators (EVPLAs) in the Day-Ahead (DA) and Real-Time (RT) markets.

As shown in Table 1, different aspects of the optimal scheduling of active distribution system problems have been studied: 1) the first group

Nomenclature

Abbreviation

ADS	Active Distribution System
ARIMA	Autoregressive Integrated Moving Average
CIC	Customer Interruption Cost
DA	Day-Ahead
DER	Distributed Energy Resource
DG	Distributed Generation
DLC	Direct Load Control
DRA	Demand Response Aggregator
DRP	Demand Response Program
ENSC	Energy Not Supplied Costs
ESS	Electrical energy Storage System
EVPLA	plug-in hybrid Electric Vehicle Parking Lot Aggregator
IC	Industrial Consumer
MILP	Mixed Integer Linear Programming
PBDRC	Price-Based Demand Response Commitment
PBRC	Price-Based Resource Commitment
PHEV	Plug-in Hybrid Electrical Vehicle
PV	Photovoltaic
RT	Real-Time
TOU	Time-Of-Use
WT	Wind Turbine

Parameters

λ	The price of electrical variables that is determined by the ADS to transact active power, reactive power, and spinning reserve with the DRA.
ρ	The price of electrical variables that is determined by the ADS to transact active power, reactive power, and spinning reserve with the EVPLA.
T	Optimization horizon.
ζ	The parameter that determines the number of additional constraints and variables that should be added to the problem in order to linearize the AC load flow equations.

Sets

Ω^{SDA}	Set of day-ahead operating scenario.
Ω^{DER}	Set of distributed energy resources facilities.
Ω^{TOU}	Set of time-of-use alternatives.
Ω^{DRA}	Set of demand response aggregators.
Ω^{EVPLA}	Set of plug-in hybrid Electric Vehicle Parking Lot Aggregators.
$\Omega^{SEVPLAS}$	Set of plug-in hybrid electric vehicle parking lot aggregator operating scenarios.
Ω^{SRT}	Set of real-time operating scenarios that are estimated in the day-ahead horizon.
Ω^{CONT}	Set of distribution contingencies.
Ω^{RT}	Set of real-time operating state.
Ω^{DLC}	Set of direct load control alternatives.
Ω^{SOLD}	Set of active power, reactive power, and spinning reserve that are sold to the wholesale market.
$\Omega^{Purchased}$	Set of active power, reactive power, and spinning reserve that are purchased from the wholesale market.
$\Omega^{Customers}$	Set of distribution system customers.
T	Set of time intervals.

Variables

$f_{n\ Load}$	Normal probability density function of load.
σ_{load}	Standard deviation of load.
μ_{load}	Mean value of load.
x	Random variable of load.
P	Active power.
SR	Spinning reserve.
RR	Regulating reserve.
Q	Reactive power.
Λ_{DRA}^{ADS}	Binary decision variable for the commitment of direct load control.
Λ_{DRA}^{IC}	Binary decision variable for the commitment of industrial customers demand response alternative.
Λ_{EVPLA}	Binary decision variable for energy selling of EVPLA.
π	Probability of scenario.
Λ_{Sold}	Binary decision variable for energy and ancillary services that are sold to wholesale market.
$\Lambda_{Purchased}$	Binary decision variable for energy and ancillary services that are purchased from the wholesale market.
C	Cost.
Λ_{DER}	Binary decision variable for DER commitment.

only considers the optimal scheduling of the distributed energy resources; 2) the second group optimizes the scheduling of distributed energy resources and the system topology.

Ref. [1] proposed a two-stage optimization process that considered the uncertainties of load, electricity price, intermittent electricity generation, and device failures. The first stage of the optimization algorithm minimized the costs of the system in normal operating conditions. The second stage minimized the load reduction in the contingent conditions. The particle swarm optimization process was used to optimize the problem. Ref. [2] presented a three-layer optimization framework that modeled the optimal commitment of distributed generation facilities and the time-of-use demand response process. The first layer minimized the distribution system's power loss, and the second layer optimally dispatched the downward microgrids. Finally, an optimal re-dispatch process was implemented to reduce the unbalance of power generation of the distribution system. The simulation process was carried out for a real distribution system. Refs. [1–2] did not model the real-time market and the arbitrage processes of DRAs and EVPLAs.

Ref. [3] introduced a multi-objective optimization process for an active distribution system considering the uncertainty of renewable electricity generation. The objective functions minimized the system

operating cost, adjustment of the active power outputs, total active power loss, and total voltage deviations. The optimization process utilized a simulated annealing algorithm integrated into the multi-objective evolutionary algorithm. However, the proposed model did not consider energy resource aggregators' real-time market and arbitrage process.

Ref. [4] assessed the day-ahead, intra-day, and real-time optimal scheduling algorithms. The day-ahead optimization process optimized the reserve margin; meanwhile, the intraday optimization algorithm optimally dispatched the available energy resources based on the updated electricity generation forecasts. Finally, the real-time optimization process minimized the deviations of electricity generations and consumption using the predictive control model. The proposed model did not consider the arbitrage processes of DRAs and EVPLAs.

Ref. [5] presented a two-stage optimization algorithm for the day-ahead horizon. The heating, ventilation, air-conditioning systems, and electric vehicles of office buildings were optimally dispatched at the first stage. At the second stage, the energy resources of the system and flexible loads were scheduled for the day-ahead horizon. Ref. [6] introduced an algorithm for optimal scheduling of active distribution system that utilized DERs and transacted energy with its downward

Table 1
Comparative study.

References		1	2	3	4	5	6	7	8	9	10	11	12	13	14	15	16	17	18	19	20	21	Proposed Approach
	Arbitrage processes of DRAs	×	×	×	×	×	×	×	×	×	×	×	×	×	×	×	×	×	×	×	×	×	✓
	Arbitrage processes of EVPLAs	×	×	×	×	×	×	×	×	×	×	×	×	×	×	×	×	×	×	×	×	×	✓
	Switching of system	×	×	×	×	×	×	×	×	×	×	×	×	×	×	×	✓	✓	✓	✓	✓	✓	✓
	Ancillary service provided by DRAs	×	×	×	×	×	×	×	×	×	×	×	×	×	×	×	×	×	×	×	×	×	✓
	Ancillary service provided by EVPLAs	×	×	×	×	×	×	×	×	×	×	×	×	×	×	×	×	×	×	×	×	×	✓
Method	MILP	×	×	×	×	×	✓	✓	×	×	×	×	×	✓	×	✓	×	×	×	×	×	×	×
	MINLP	×	✓	×	×	×	×	×	×	×	✓	✓	×	×	×	×	×	×	×	×	×	×	✓
	Heuristic	✓	×	✓	✓	✓	×	×	✓	✓	×	×	✓	×	✓	×	✓	✓	✓	✓	✓	✓	✓
Model	Deterministic	✓	✓	✓	✓	✓	✓	✓	×	✓	×	×	✓	×	✓	×	✓	✓	✓	×	×	×	×
	Stochastic	×	×	×	×	×	×	×	✓	×	×	✓	×	✓	×	✓	×	×	×	×	✓	✓	✓
Objective Function	Revenue	×	×	×	×	×	✓	×	×	×	×	×	✓	×	×	×	×	×	×	×	✓	✓	✓
	Gen. Cost	✓	✓	✓	✓	✓	✓	✓	✓	✓	✓	✓	✓	✓	✓	✓	✓	✓	✓	✓	✓	✓	✓
	Storage Cost	✓	✓	×	×	×	✓	×	×	×	×	×	×	×	×	×	✓	×	×	✓	✓	✓	✓
	Security Costs	✓	×	×	✓	×	✓	×	✓	×	×	×	×	×	×	×	×	×	×	×	✓	✓	✓
	PHEV cost	×	×	×	×	✓	✓	×	✓	×	×	×	×	✓	×	×	×	×	✓	×	✓	✓	✓
	DRP costs	✓	✓	✓	×	✓	✓	✓	✓	✓	×	×	×	✓	×	×	×	×	✓	✓	✓	✓	✓
	WT	✓	✓	×	×	×	✓	✓	×	✓	×	×	✓	×	✓	×	✓	×	×	✓	✓	✓	✓
	PV	✓	✓	×	×	×	✓	✓	×	✓	×	×	✓	×	✓	×	✓	×	×	✓	✓	✓	✓
	DA-Market scheduling	✓	✓	✓	✓	✓	✓	✓	✓	✓	✓	✓	✓	✓	✓	✓	✓	✓	✓	✓	✓	✓	✓
	RT- Market scheduling	×	×	×	✓	×	×	×	×	×	×	✓	×	×	×	×	×	×	×	×	✓	✓	✓
Uncertainty Model	PHEV	×	×	×	×	×	✓	×	×	×	×	×	×	✓	×	×	×	×	✓	×	✓	✓	✓
	DRP	×	×	×	×	×	✓	×	×	×	×	×	×	×	×	×	×	×	✓	×	✓	✓	✓
	DA Market price	✓	×	×	×	×	✓	×	×	×	×	×	×	×	×	×	×	×	×	×	✓	✓	✓
	RT Market price	×	×	×	×	×	×	×	×	×	×	×	×	×	×	×	×	×	×	×	✓	✓	✓
	Contingency	✓	×	×	×	×	×	✓	×	×	×	×	×	×	×	×	×	×	×	×	✓	✓	✓
	Loads	✓	×	×	×	×	✓	×	×	×	✓	×	×	×	×	×	×	×	×	×	✓	✓	✓
	Inter. Electricity generation	✓	✓	✓	×	×	✓	✓	✓	×	×	✓	×	✓	×	✓	×	✓	×	×	✓	✓	✓

energy hubs. The model compromised a two-level optimization process. At the first level, the optimal scheduling of distribution system resources was determined, and the energy procurement cost was minimized. The second level problem minimized the operating costs of energy hubs. The proposed model used a linear optimization process and reduced the system costs by about 82.2%. Refs. [5–6] did not model the real-time market and the arbitrage processes of DRAs and EVPLAs.

Ref. [7] evaluated a two-stage optimization process for optimal scheduling of distributed energy resources of a distribution system. At the first stage, the process minimized the energy imports and maximized the energy exports for the day-ahead horizon. At the second stage, the process minimized the energy deficits and maximized the energy surplus for the real-time horizon. Ref. [8] presented an optimization framework to schedule the system resources for the day-ahead horizon considering the air pollution and congestion of the electrical system. The algorithm utilized the grey wolf optimization process to optimize the mixed-integer non-linear programming model. Refs. [7–8] did not consider the arbitrage processes of DRAs and EVPLAs and the switching process of the distribution system.

Ref. [9] introduced a three-layer optimization algorithm that considered multiple stockholders. At the first layer, the optimal energy consumption of consumers was determined. At the second layer, the scheduling of microgrids was optimized. Finally, the distribution system optimal scheduling was carried out at the third layer. The primal–dual interior-point method was utilized to optimize the model. The proposed model did not consider the switching process of the active distribution system and the arbitrage mechanisms of DRAs and EVPLAs. Ref. [10] evaluated a dual-horizon optimization process for active distribution system management. At the first stage, the optimal energy imports and exports were determined. At the second stage, the distributed energy resources and energy storage facilities were dispatched to minimize the energy generation and consumption mismatches. The uncertainties of energy generations and consumption were modeled. The model did not consider the real-time market and the arbitrage processes of DRAs and EVPLAs. Ref. [11] presented a two-stage stochastic optimization approach for optimal scheduling of distribution system resources for the day-ahead and real-time horizons. The model considered the level of risk exposure and the uncertainties of load and wind power generation. The CONOPT 4 solver optimized the mixed-integer non-linear optimization model. The 33-bus IEEE test system cost was reduced by about 19.9%. The proposed model did not consider the switching of the active distribution system and the arbitrage process of distributed energy resources aggregators.

Ref. [12] presented a two-stage multi-objective optimization process for optimal scheduling of distribution system using particle swarm optimization-bacterial foraging algorithm. The model considered peak-valley load difference, voltage deviation, and power loss as objective functions. At the first stage, the Pareto solutions were found, and at the second stage, the optimal scheduling of system resources was determined using the entropy weight decision-making method. Ref. [13] introduced a day-ahead stochastic optimization framework for optimal scheduling of distribution system compromised renewable energy resources, parking lots, and conventional energy resources. The demand response programs, electric vehicles' uncertainties, and intermittent electricity generation were modeled. The proposed model was solved by mixed-integer linear programming. Refs. [12–13] did not model the switching of the active distribution system and the arbitrage process of distributed energy resources aggregators.

Ref. [14] proposed an optimization process to schedule the battery energy storage and distributed generation system considering power quality constraints of a distribution system. The objective function considered the power loss of the system. The particle swarm optimization was utilized to optimize the problem. The introduced model reduced the system loss of the 123-bus test system by about 3.86%. Ref. [15] introduced a robust optimization procedure for optimal dispatching of distribution system resources considering single-phase distributed generations. The problem was decomposed into two sub-problems, and the model considered the lower and upper bounds of optimization space using the cutting plane algorithm. The proposed method reduced the voltage deviations of the 123-bus system by about 2.3%. Refs. [14–15] did not model the arbitrage process of distributed energy resources aggregators and the switching mechanism of the active distribution system.

Based on the above categorization and for the second category of papers, Ref. [16] introduced a mixed-integer non-linear programming optimization algorithm for optimal day-ahead scheduling of distributed energy resources and switching of system switches. The proposed method utilized a genetic algorithm for the optimization process. Ref. [17] proposed a mixed-integer dynamic optimization process to minimize distribution system costs by switching tap changers, capacitors, and energy storage facilities. The renewable energy generation facilities and distributed generation systems were considered in the model. The introduced method reduced the computational burden and costs of the system by about 91.28% and 0.06%, respectively. Refs. [16–17] did not consider the arbitrage of energy resources aggregators and the optimal real-time scheduling of distribution system resources.

Ref. [18] introduced a multi-objective optimization framework to schedule distribution system distributed generation facilities, controllable loads, coordinated electric vehicle charge/discharge process, and system topology. Ref. [18] did not consider the arbitrage processes of DRAs and EVPLAs. Ref. [19] proposed an optimization algorithm for the day-ahead and hourly scheduling of the energy resources and system topology. The hourly reconfiguration of the system was considered in the optimization process, and the non-linear model was solved by particle swarm optimization. The model considered the energy loss cost, switching cost of remote switches, electricity costs purchased from distributed generation, electricity costs purchased from the wholesale market, and demand response costs. The proposed model reduced the system costs by about 8.32%. Ref. [20] presented a six-level optimization process for optimal scheduling of the distribution system in the day-ahead and real-time horizons. The risk-averse bidding strategy of the system for the normal and contingent conditions was modeled, and the energy transactions between the system and active microgrids were considered. The multi-level optimization processes were optimized using parallel genetic algorithm, DICOPT, and CPLEX solver of GAMS. The introduced method increased the revenue of the ADS by about 3.17%. Refs. [19–20] did not consider distributed energy resource aggregators' arbitrage process.

Ref. [21] proposed a framework to simulate the day-ahead and real-time pre-event preventive and post-event corrective actions for contingent conditions. The optimal day-ahead scheduling was determined at the first stage using robust optimization. The optimal real-time market scheduling was carried out at the second stage. Finally, at the third stage, different contingent conditions were considered. However, the model did not consider distributed energy resource aggregators' arbitrage process.

Table 1 shows a comparative study between the current framework and the frameworks proposed in other studies. An algorithm that simultaneously considers the arbitrage strategies of the active distribution system, plug-in hybrid electric vehicle parking lot aggregators, and demand response aggregators in the day-ahead and real-time horizons is less frequent in the previous papers. Further, the proposed method models the optimal switching of electrical system switches in the day-ahead and real-time markets to reduce the impacts of contingencies.

The main contributions of this paper are as follows:

- The proposed algorithm considers the arbitrage strategy of electric vehicle parking lot aggregators and demand response aggregators that sell energy and ancillary services to the distribution system in the day-ahead and real-time markets.
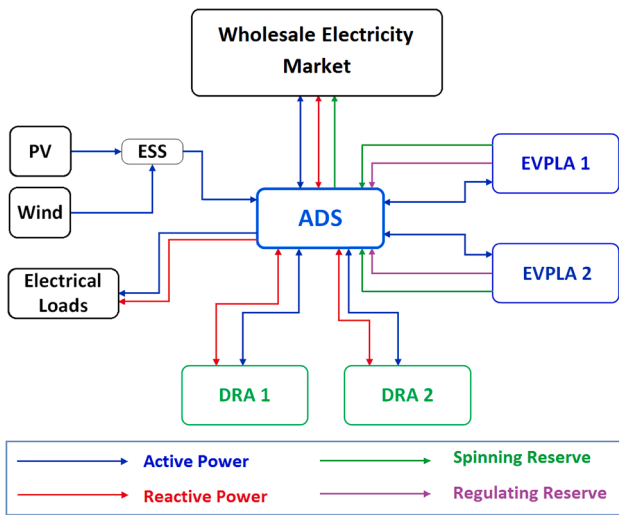
Fig. 1. The active power and ancillary services transactions between ADS and distributed energy resources in the day-ahead and real-time markets.

- The arbitrage strategy of the distribution system operator that sells the energy and ancillary service to the wholesale electricity market is modeled.
- The following uncertainties of the system are considered: 1) electrical demand; 2) wind turbine and photovoltaic electricity generation; 3) demand response aggregators' contribution scenarios; 4) plug-in hybrid electric vehicle aggregators' contribution scenarios; 5) contingency scenarios; and 6) day-ahead and real-time market prices.
- The optimization process switches the distribution system electrical switches in the day-ahead and real-time contingent conditions to reduce the costs of energy not supplied.

- The robust and lexicographic ordering optimization methods are utilized to find the optimal values of the conflicting objective functions.

The rest of this paper is organized as follows. The proposed framework is formulated in Section 2. In Section 3, the solution algorithm is introduced, and the simulation results of the 70-bus test system are assessed in Section 4. Finally, conclusions are presented in Section 5.

2. Problem modeling and formulation

As shown in Fig. 1, the active distribution system transacts energy and ancillary services with the wholesale electricity market in the day-ahead and real-time markets and supplies its downward electrical loads. Further, the ADS can sell electricity to the EVPLAs and DRAs in the day-ahead and real-time markets. The EVPLAs and DRAs can sell their energy and ancillary services to the ADS. The operational scheduling of ADS consists of determining the commitment schedule of the distribution system distributed energy resources, EVPLAs, and DRAs in the day-ahead and real-time markets.

2.1. The proposed framework

A two-level optimization algorithm is presented, as shown in Fig. 2. The first stage of the first-level optimization problem maximizes the day-ahead profit of DRAs and EVPLAs. At the second stage of the first level problem, the ADS operator maximizes its net revenue for the day-ahead scheduling horizon, minimizing the energy not supplied costs. The ADS operator should consider the strategic behavior of DRAs and EVPLAs. At the second level problem, the ADS operator maximizes its net revenue for the real-time scheduling horizon, minimizing the mismatch of control variables and the expected Customer Interruption Costs (CICs).

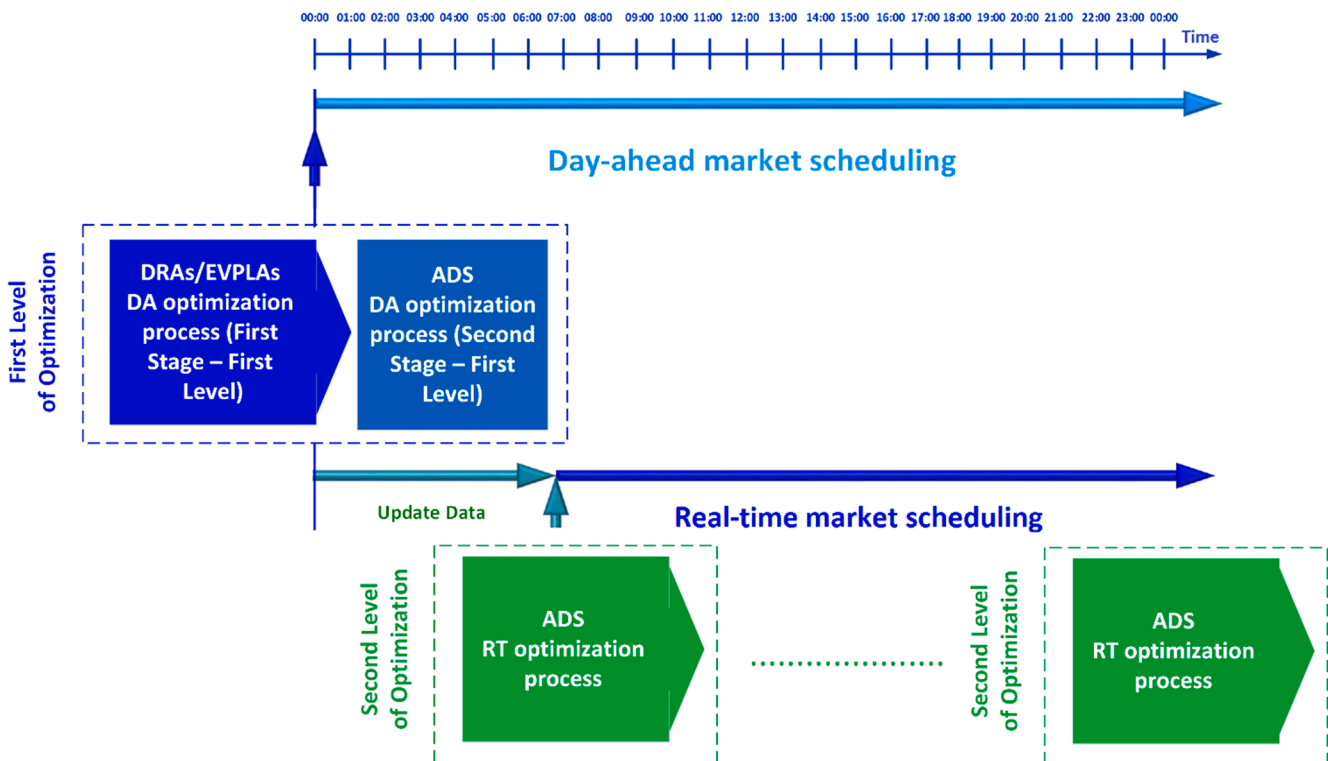(A) *The Uncertainty of System*

Fig. 2. The proposed optimization process for day-ahead and real-time horizons.

The uncertainties of the input variables and parameters of active distribution system distributed energy resources, EVPLAs, and DRAs should be modeled in the problem. The ADS has multiple uncertainties sources in the day-ahead and real-time scheduling horizons that can be categorized into the following groups:

1) Wind turbine and photovoltaic electricity generation; 2) electrical demand; 3) demand response aggregators' contribution scenarios; 4) plug-in hybrid electric vehicle aggregators' contribution scenarios; 5) contingency scenarios; and 6) day-ahead and real-time market prices.

The ARIMA models generate scenarios for market prices; the Monte Carlo simulation provides contingency scenarios [20,21]. The Normal probability density function is utilized to model the uncertainty of loads that can be presented as (1) [22]:

$$f_{n\ Load}(x) = \frac{1}{\sigma_{load}\sqrt{2\pi}}e^{-\left[\frac{(x-\mu_{load})^2}{2\sigma_{load}^2}\right]} \tag{1}$$

where μ_{load} and σ_{load} are the mean values of load and standard deviation of load, respectively. Further, x is the random variable of the load. The model of electricity generation of wind turbine and photovoltaic systems are available in [20] and are not presented for the sake of space.

(B) *Modeling of Demand Response Aggregators*

The arbitrage strategy of DRAs and EVPLAs may reduce the availability of ADS control variables in normal and contingent conditions. Thus, at the first stage of the first level optimization process, the system operator simulates the ADS should consider the arbitrage strategy of DRAs and EVPLAs using Price-Based Demand Response Commitment (PBDRC) and Price-Based Resource Commitment (PBRC) simulation processes, respectively. It is assumed that the DRA aggregates the demand responses of the Industrial Consumers (ICs), performs the PBDRC procedure, and adopts an optimal arbitrage strategy for selling the demand response alternatives [23]. The PBDRC is a profit maximization problem that the objective function of each DRA can be formulated as (2):

$$Max\ \mathfrak{M}_{\Lambda_{DRA}^{ADS},\Lambda_{DRA}^{IC}} = (\sum_T \lambda_{Sold}^{Active\ DLC}\cdot P^{DRA\ DLC} + \sum_T \lambda_{Sold}^{DRA\ SR}\cdot SR^{DRA\ DLC} + \sum_T \lambda_{Sold}^{Reactive\ DLC}\cdot Q^{DRA\ DLC})\cdot\Lambda_{DRA}^{ADS}$$
$$-(\sum_T \lambda_{Purchased}^{Active\ DLC}\cdot P^{IC\ DLC} + \sum_T \lambda_{Purchased}^{DRA\ SR}\cdot SR^{IC\ DLC} + \sum_T \lambda_{Purchased}^{Reactive\ DLC}\cdot Q^{IC\ DLC})\cdot\Lambda_{DRA}^{IC} \tag{2}$$

where *P, SR* and *Q* are active power, spinning reserve, and reactive power, respectively. The λ parameter is the price of active power, reactive power, and spinning reserve determined by the ADS to transact these quantities with the DRA. Further, Λ_{DRA}^{ADS}, Λ_{DRA}^{IC} are the binary decision variables for the commitment of direct load control and industrial customers demand response alternatives, respectively. The *T* parameter is the optimization horizon that are 24 h and 15 min for the day-ahead and real-time markets, respectively.

The PBDRC objective function consists of the following terms that are provided by Direct Load Control (DLC) processes: 1) the revenue of active power sold to the ADS ($\sum_T \lambda_{Sold}^{Active\ DLC}\cdot P^{DRA\ DLC}$); 2) the revenue of spinning reserve sold to the ADS ($\sum_T \lambda_{Sold}^{DRA\ SR}\cdot SR^{DRA\ DLC}$); 3) the revenue of reactive power sold to the ADS ($\sum_T \lambda_{Sold}^{Reactive\ DLC}\cdot Q^{DRA\ DLC}$); 4) the cost of active power purchased from the ICs ($\sum_T \lambda_{Purchased}^{Active\ DLC}\cdot P^{IC\ DLC}$); 5) the cost of spinning reserve purchased from ICs ($\sum_T \lambda_{Purchased}^{DRA\ SR}\cdot SR^{IC\ DLC}$); 6) the cost of reactive power purchased from ICs ($\sum_T \lambda_{Purchased}^{Reactive\ DLC}\cdot Q^{IC\ DLC}$).

Eq. (2) is subjected to each bus's maximum available active and reactive load commitment of the ADS and ICs. The DRA can utilize an arbitrage strategy to maximize its revenue, and it can supply active/reactive load by local generation or purchase active/reactive power from the ADS.

(C) *Modeling of Plug-in Hybrid Electric Vehicle Aggregators*

As shown in Fig. 2, at the first stage of the first level optimization process, the system operator should simulate the arbitrage strategy of EVPLAs using the PBRC simulation process. The EVPLA can purchase electricity from ADS and sell the energy and ancillary services to the ADS. The EVPLA can sell regulating and spinning reserves to the ADS in the day-ahead market. Further, it can sell the regulating reserve to the ADS in the real-time market. The EVPLA can aggregate PHEVs' charging/discharging patterns, perform the PBRC process, and adopt an arbitrage strategy [23].

The objective function of PBRC can be formulated as (3):

$$Max\ \mathfrak{A}_{\Lambda_{EVPLA}} = [(\sum_T \rho_{Sold}^{Energy}\cdot P^{EVPLA} + \sum_T \rho_{Sold}^{RR}\cdot RR^{EVPLA} + \sum_T \rho_{Sold}^{SR}\cdot SR^{EVPLA})\cdot\Lambda_{EVPLA} -$$
$$\sum_T \rho_{Purchased}^{Energy}\cdot P^{EVPLA}\cdot(1-\Lambda_{EVPLA})] \tag{3}$$

$$P_b^{EVPLA}\cdot\Lambda_{EVPLA}\leqslant P_b^{EVPLA\ Max}$$
$$\forall\ b\in Buses \tag{4}$$

$$RR_b^{EVPLA}\cdot\Lambda_{EVPLA}\leqslant RR_b^{EVPLA\ Max}$$
$$\forall\ b\in Buses \tag{5}$$

$$SR_b^{EVPLA}\cdot\Lambda_{EVPLA}\leqslant SR_b^{EVPLA\ Max}$$
$$\forall\ b\in Buses \tag{6}$$

where *P, RR*, and *SR* are active power, regulating reserve, and spinning reserve, respectively. The ρ parameter is the price of active power, regulating reserve, and spinning reserve determined by the ADS to transact these quantities with the EVPLA. Further, Λ_{EVPLA} is the binary decision variable for energy selling of EVPLA. The PBRC objective function compromises the following terms: 1) the revenue of active

power sold to the ADS ($\sum_T \rho_{Sold}^{Energy} \cdot P^{EVPLA}$); 2) the revenue of regulating reserve sold to the ADS ($\sum_T \rho_{Sold}^{RR} \cdot RR^{EVPLA}$) ; 3) the revenue of spinning reserve sold to the ADS ($\sum_T \rho_{Sold}^{SR} \cdot SR^{EVPLA}$); 4) the cost of active power purchased by the EVPLA ($\sum_T \rho_{Purchased}^{Energy} \cdot P^{EVPLA}$).

Eq. (3) is subjected to the constraints of the maximum available EVPLA resource commitment of each bus that are presented as (4)-(6)

$$
\begin{aligned}
Max \; \mathbb{F}_1^{DA} \Lambda_{Sold}, \Lambda_{Purchased}, \Lambda_{DER}, \Lambda_{DRA}^{ADS}, \Lambda_{DRA}^{IC} = &\sum_{s1\in\Omega^{SDA}} \pi_{s1}[(\gamma_{Active\_Sold}^{DA}\cdot P_{Sold}^{DA\;WM} + \gamma_{Reactive\_Sold}^{DA}\cdot Q_{Sold}^{DA\;WM} + \gamma_{SR\_Sold}^{DA}\cdot SR_{Sold}^{DA\;WM})\cdot\Lambda_{Sold} \\
&-(\gamma_{Active\_Purchased}^{DA}\cdot P_{Purchased}^{DA\;WM} + \gamma_{Reactive\_Purchased}^{DA}\cdot Q_{Purchased}^{DA\;WM})\cdot\Lambda_{Purchased} - \sum_{\Omega^{DER}} C^{DER}\cdot\Lambda_{DER} \\
&-\sum_{\Omega^{TOU}}\sum_{s2\in\Omega^{DRA}}\pi_{s2}\cdot C_{TOU}^{DRA} - \sum_{\Omega^{DLC}}(C_{DLC}^{DRA}\cdot\Lambda_{DRA}^{ADS} + C_{DLC}^{IC}\cdot\Lambda_{DRA}^{IC}) - \sum_{\Omega^{EVPLA}}\sum_{s3\in\Omega^{SEVPLAS}}\pi_{s3}\cdot\rho_{Purchased}^{Energy\;DA}\cdot P^{EVPLA} \\
&-\sum_{\Omega^{EVPLA}}\sum_{s3\in\Omega^{SEVPLAS}}\pi_{s3}\cdot\rho_{Purchased}^{RR\;DA}\cdot RR^{EVPLA} - \sum_{\Omega^{EVPLA}}\sum_{s3\in\Omega^{SEVPLAS}}\pi_{s3}\cdot\rho_{Purchased}^{SR\;DA}\cdot SR^{EVPLA} \\
&+\sum_{\Omega^{EVPLA}}\sum_{s4\in\Omega^{SEVPLAP}}\pi_{s4}\cdot\rho_{Sold}^{Energy\;DA}\cdot P^{EVPLA} + \sum_{s5\in\Omega^{SRT}}\pi_{s5}\cdot\Xi^{RT}]
\end{aligned}
\tag{7}
$$

constraints. Eq. (4) presents the maximum constraint of the active power of EVPLA. Eq. (5) and Eq. (6) present the maximum constraints of regulating reserve and spinning reserve, respectively.

(D) *Modeling of Arbitrage*

The objective of the distribution system operator for the arbitrage process is profit maximization by identifying arbitrage opportunities and optimal bidding in the day-ahead and real-time markets. Arbitrage is the process of earning riskless profits by taking advantage of differential pricing for the same physical asset or security [24]. The distribution system operator can utilize the arbitrage strategy for active power, reactive power, and reserve markets when the energy and ancillary services prices are different in the scheduling horizon. The ADS can purchase the energy and ancillary services when their prices are low and sell them when their prices are high [24]. Three assumptions are considered for the arbitrage strategy of the distribution system operator. First, the ESSs are utilized to perform this strategy. Second, the system operator estimates the system load and the price of energy and ancillary services of the wholesale market. Then, the system operator performs the PBDRC and PBRC optimization processes and estimates the optimal contribution scenarios of the DRAs of EVPLAs. The system operator optimizes the control variables of the system for the day-ahead and real-time markets. Third, the optimization procedure considers the contingency scenarios of the system and changes the scheduling of system resources and switches. Fig. 3 presents the arbitrage strategy implementation of ADS operator for the energy and ancillary services market.

As shown in Fig. 3, when the price of the spinning reserve market is higher than the energy market price, the arbitrage process between energy and spinning reserve service can be performed. The maximum capability of dispatchable system DERs can be traded in the spinning reserve market, and the rest of the system DERs capacity can be allocated to the energy market [24]. If the DERs reactive power injection cost is lower than the price of the reactive power market, then the maximum absorption of DERs reactive power can be traded with the reactive power market. Finally, when the price of the reactive power market is much lower than that of the energy and spinning reserve markets, then the active power generation of DERs is much more profitable than the reactive power generation for the ADS. Thus, the maximum capacity of DERs is traded in the energy and spinning reserve markets, and the maximum apparent power limits the reactive power injection of DERs [24].

(E) *Objective Function of Day-ahead Scheduling*

As shown in Fig. 2, at the second stage of the first level problem, the system operator should maximize its net revenue for the DA scheduling horizon; meanwhile, it should minimize the energy not supplied costs. The first objective function of the DA scheduling can be formulated as (7):

where π, P, Q, SR are the probability of scenario, active power, reactive power, and spinning reserve, respectively. The γ parameter is the price of active power, regulating reserve, and spinning reserve determined by the wholesale market to transact these quantities with the ADS. Λ_{Sold} is the binary decision variable for energy and ancillary services sold to the wholesale market. $\Lambda_{Purchased}$ is the binary decision variable for energy and ancillary services purchased from the wholesale market. Λ_{DER} is the binary decision variable for DER commitment.

The first objective function of day-ahead scheduling compromises the expected values of the following terms: 1) the revenue of active power sold to the day-ahead wholesale market ($\gamma_{Active\_Sold}^{DA}\cdot P_{Sold}^{DA\;WM}$); 2) the revenue of reactive power sold to the day-ahead wholesale market ($\gamma_{Reactive\_Sold}^{DA}\cdot Q_{Sold}^{DA\;WM}$); 3) the revenue of spinning reserve sold to the day-ahead wholesale market ($\gamma_{SR\_Sold}^{DA}\cdot SR_{Sold}^{DA\;WM}$); 4) the cost of active power purchased from the day-ahead wholesale market ($\gamma_{Active\_Purchased}^{DA}\cdot P_{Purchased}^{DA\;WM}$); 5) the cost of reactive power purchased from the day-ahead wholesale market ($\gamma_{Reactive\_Purchased}^{DA}\cdot Q_{Purchased}^{DA\;WM}$); 6) the cost of DER commitment ($\sum_{\Omega^{DER}} C^{DER}\cdot\Lambda_{DER}$); 7) the cost of DRA Time-Of-Use (TOU) implementation ($\sum_{\Omega^{TOU}}\sum_{s2\in\Omega^{DRA}}\pi_{s2}\cdot C_{TOU}^{DRA}$); 8) the cost of DRA and IC direct load commitment ($\sum_{\Omega^{DLC}}(C_{DLC}^{DRA}\cdot\Lambda_{DRA}^{ADS} + C_{DLC}^{IC}\cdot\Lambda_{DRA}^{IC})$); 9) the cost of energy purchased from EPVLAs in the day-ahead market ($\sum_{\Omega^{EVPLA}}\sum_{s3\in\Omega^{SEVPLAS}}\pi_{s3}\cdot\rho_{Purchased}^{Energy\;DA}\cdot P^{EVPLA}$); 10) the cost of regulating reserve purchased from EPVLAs in the day-ahead market ($\sum_{\Omega^{EVPLA}}\sum_{s3\in\Omega^{SEVPLAS}}\pi_{s3}\cdot\rho_{Purchased}^{RR\;DA}\cdot RR^{EVPLA}$); 11) the cost of spinning reserve purchased from EPVLAs in the day-ahead market ($\sum_{\Omega^{EVPLA}}\sum_{s3\in\Omega^{SEVPLAS}}\pi_{s3}\cdot\rho_{Purchased}^{SR\;DA}\cdot SR^{EVPLA}$); 12) the revenue of energy sold to the EVPLAs in the day-ahead market ($\sum_{\Omega^{EVPLA}}\sum_{s4\in\Omega^{SEVPLAP}}\pi_{s4}\cdot\rho_{Sold}^{Energy\;DA}\cdot P^{EVPLA}$); and 13) the estimated value of real-time operational scheduling objective function revenues and costs terms that are calculated in the real-time optimization process ($\sum_{s5\in\Omega^{SRT}}\pi_{s5}\cdot\Xi^{RT}$).

The ADS cannot simultaneously purchase and sell energy from/to the wholesale market.

The second objective function of DA scheduling of ADS can be formulated as (8):

$$
Min \; \mathbb{F}_2^{DA} = \sum_{s1\in\Omega^{SDA}}\pi_{s1}\sum_{s6\in\Omega^{CONT}}\pi_{s6}.ENSC
\tag{8}
$$

The second objective function consists of Energy Not Supplied Costs
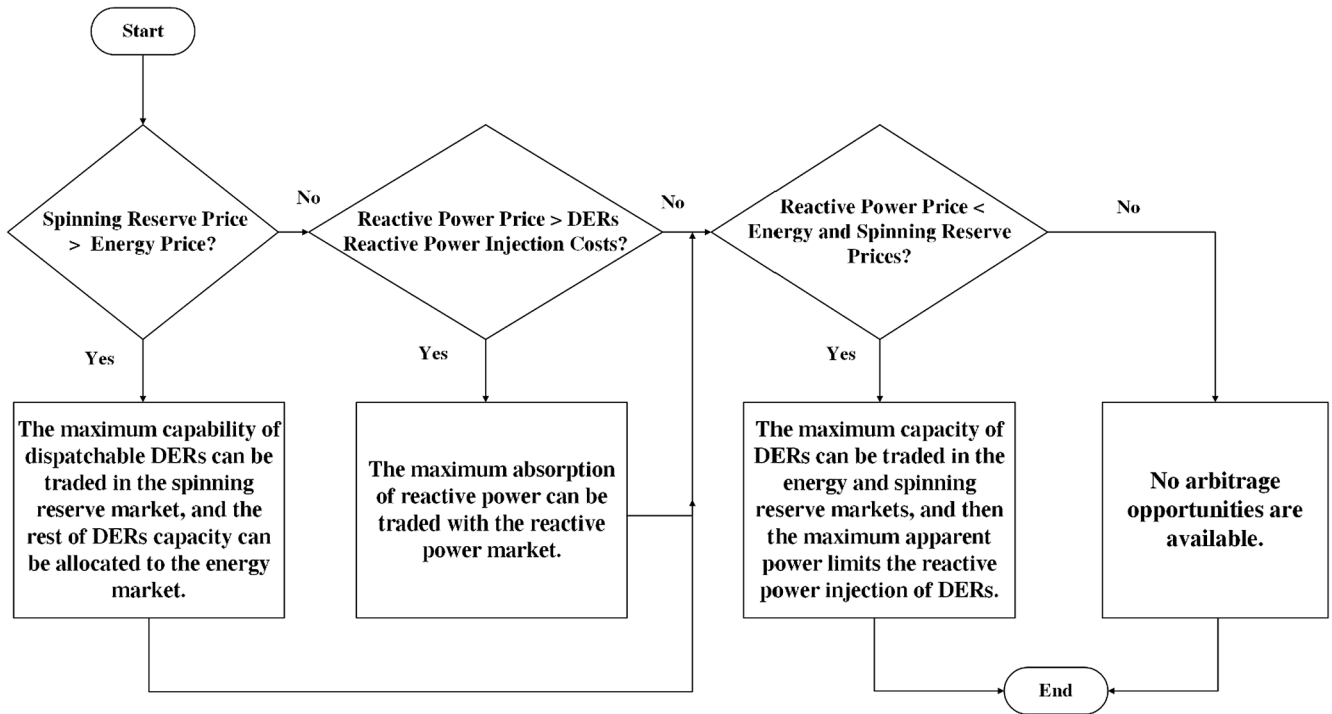
Fig. 3. The arbitrage strategy implementation of ADS operator for the energy and ancillary services market.

(ENSC) for different contingency scenarios. The first and second objective functions are conflicting because higher reliability levels may require more commitment of DERs and DRAs resources.

The linearization technique is adopted to linearize (7) and (8). The day-ahead scheduling of ADS is constrained by the following constraints:

(1) *Minimum and maximum operating limits of facilities*

The minimum and maximum operating limits of ESSs, electrical energy generating devices, network facilities, and DRA operating limits.

(2) *Ramp rates and minimum up/downtime of electrical energy generating and storage systems*

The limits of ramp up, ramp down, minimum up/downtime of electrical energy generating systems are considered in the optimization procedure. Further, the limits of ramp up and ramp down of energy storage are considered. Ref. [25] is used for the linearization of ramp-up/down limitations.

(3) *The load flow constraints*

The non-linear AC load flow constraints of the distribution system are considered. The linearization of the AC load flow is accomplished employing the proposed method of Ref. [26].

(F) *Objective Function of Real-time Scheduling*

As shown in Fig. 2, at the second level problem, the ADS operator should maximize his/her net revenue for the real-time scheduling horizon; meanwhile, he/she should minimize the mismatch of the optimal day-ahead scheduled control variables, the real-time control variables, and the expected CICs. At the real-time horizon, the look-ahead method is applied as defined in [27]. The optimization process is carried out every 15 min with updated data. The accepted values of distributed energy aggregators spinning reserve bids in the day-ahead market should be controlled as fixed parameters in the real-time market. Any deviation of ancillary services is penalized by the active distribution system operator. Thus, the RT objective function can be presented as (9):

$$
\begin{aligned}
Max \ \mathbb{S}^{RT} = & \sum_{s7 \in \Omega^{CONT}} \pi_{s7} \cdot \Big[\sum_{\Omega^{RT}} \big((\gamma_{Active\_Sold}^{RT} \cdot P_{Sold}^{RT \ WM} + \gamma_{Reactive\_Sold}^{RT} \cdot Q_{Sold}^{RT \ WM} + \gamma_{SR\_Sold}^{RT} \cdot SR_{Sold}^{RT \ WM}) \\
& - (\gamma_{Active\_Purchased}^{RT} \cdot P_{Purchased}^{RT \ WM} + \gamma_{Reactive\_Purchased}^{DA} \cdot Q_{Purchased}^{RT \ WM}) \big) - \sum_{\Omega^{DER}} \Delta C^{DER} - \sum_{\Omega^{TOU}} \Delta C_{TOU}^{DRA} - \sum_{\Omega^{DLC}} \Delta C_{DLC}^{DRA} \\
& - \sum_{\Omega^{EVPLA}} \rho_{Purchased}^{Energy \ RT} \cdot P^{EVPLA} - \sum_{\Omega^{EVPLA}} \rho_{Purchased}^{RR \ RT} \cdot RR^{EVPLA} - \sum_{\Omega^{EVPLA}} \rho_{Purchased}^{SR \ RT} \cdot SR^{EVPLA} + \sum_{\Omega^{EVPLA}} \rho_{Sold}^{Energy \ RT} \cdot P^{EVPLA} \\
& - \sum_{\Omega^{SOLD}} (Penalty_{Active\_Sold}^{DA \ WM} + Penalty_{Rective\_Sold}^{DA \ WM} + Penalty_{SR\_Sold}^{DA \ WM}) - \\
& \sum_{\Omega^{Purchased}} (Penalty_{Active\_Purchased}^{DA \ WM} + Penalty_{Rective\_Purchased}^{DA \ WM} + Penalty_{SR\_Purchased}^{DA \ WM}) + \sum_{\Omega^{Customers}} CIC \Big]
\end{aligned}
\tag{9}
$$

The objective function of real-time scheduling consists of the expected values of the normal condition and contingency scenarios of the following terms: 1) the revenue of active power sold to the real-time wholesale market ($\gamma_{Active\_Sold}^{RT} \cdot P_{Sold}^{RT\ WM}$); 2) the revenue of reactive power sold to the real-time wholesale market ($\gamma_{Reactive\_Sold}^{RT} \cdot Q_{Sold}^{RT\ WM}$); 3) the revenue of reserve sold to the real-time wholesale market ($\gamma_{SR\_Sold}^{RT} \cdot SR_{Sold}^{RT\ WM}$); 4) the cost of active power purchased from the real-time wholesale market ($\gamma_{Active\_Purchased}^{RT} \cdot P_{Purchased}^{RT\ WM}$); 5) the cost of reactive power purchased from the real-time wholesale market ($\gamma_{Reactive\_Purchased}^{DA} \cdot Q_{Purchased}^{RT\ WM}$); 6) the mismatch cost of DER commitment ($\sum_{\Omega^{DER}} \Delta C^{DER}$); 7) the mismatch cost of DRA TOU demand response implementation ($\sum_{\Omega^{TOU}} \Delta C_{TOU}^{DRA}$); 8) the mismatch cost of DRA DLC commitment ($\sum_{\Omega^{DLC}} \Delta C_{DLC}^{DRA}$); 9) the cost of energy purchased from EPV-LAs in real-time market ($\sum_{\Omega^{EVPLA}} \rho_{Purchased}^{Energy\ RT} \cdot P^{EVPLA}$); 10) the cost of regulating reserve purchased from EPVLAs in real-time market ($\sum_{\Omega^{EVPLA}} \rho_{Purchased}^{RR\ RT} \cdot RR^{EVPLA}$); 11) the cost of spinning reserve purchased from EPVLAs in real-time market ($\sum_{\Omega^{EVPLA}} \rho_{Purchased}^{SR\ RT} \cdot SR^{EVPLA}$); 12) the revenue of energy sold to the EVPLAs in real-time market ($\sum_{\Omega^{EVPLA}} \rho_{Sold}^{Energy\ RT} \cdot P^{EVPLA}$); 13) the cost of penalties of active power sold mismatches in the day-ahead and real-time markets ($Penalty_{Active\_Sold}^{DA\ WM}$); 14) the cost of penalties of reactive power sold mismatches in the day-ahead and real-time markets ($Penalty_{Reactive\_Sold}^{DA\ WM}$); 15) the cost of penalties of spinning reserve sold mismatches in the day-ahead and real-time markets ($Penalty_{SR\_Sold}^{DA\ WM}$); 16) the cost of penalties of active power purchased mismatches in the day-ahead and real-time markets ($Penalty_{Active\_Purchased}^{DA\ WM}$); 17) the cost of penalties of reactive power purchased mismatches in the day-ahead and real-time markets ($Penalty_{Reactive\_Purchased}^{DA\ WM}$); 18) the cost of penalties of spinning reserve purchased mismatches in the day-ahead and real-time markets ($Penalty_{SR\_Purchased}^{DA\ WM}$); and 19) the CICs ($\sum_{\Omega^{Customers}} CIC$).

The Ξ term in (7) is the estimated values of the 1–18 terms of (9). The control variables of the real-time problem are the volume of the sold active and reactive powers and spinning reserve to the wholesale market, real-time DLC implementation, real-time energy and ancillary services transactions with EVPLAs and DRAs, and status of switches. The real-time problem explores the adequacy of ADS resources in contingent conditions and switches the zonal switches for contingency scenarios. The DA problem receives the feedback of the real-time problem and reschedules the ADS DERs.

3. Solution methodology

An iterative optimization algorithm is proposed for solving the proposed problem. Fig. 4 shows the flowchart of the optimization algorithm. As shown in Fig. 4, the optimization problem is a multi-objective optimization problem that a solution ψ is dominant in another solution Θ. The solutions that are not dominated by each other are non-dominated objective functions solutions. The dominant solution can be achieved when one of the objective functions cannot increase without reducing the other objective functions. This condition is called Pareto optimality. The set of optimal solutions is called Pareto optimal solution [28]. The detailed explanations of dominant and non-dominant solutions are available in [28] and are not presented for the sake of space. The Pareto front consists of non-dominated solutions. In this paper, the augmented ε-constraint with lexicographic ordering method is proposed to solve the DA problem.

The general formulation of the ε-constraint optimization technique can be written as (10):

$$Min\left(F_1(x) - r_1 \sum_{k=2}^{K} \frac{s_k}{r_k}\right) \tag{10}$$

$$subject\ to\quad F_k(x) + s_k = e_k^z\quad \forall k = 2, ..., K;\ s_k \in R^+$$

$$e_k^z = F_k^{Max} + z_k\left(\frac{F_k^{Min} - F_k^{Max}}{q^k}\right) \tag{11}$$

$$\forall k = 2, ..., K,\ \forall z_k = 0, 1, ..., q_k$$

where $s_2, ..., s_k$ are the slack variables. Further, r_k is the optimal range of the kth objective function based on the pay-off matrix of $\left(F_k^{Max} - F_k^{Min}\right)$ [29]. The lexicographic ordering method utilizes the fuzzy membership function (μ_k^z) for the solution of X^z in the Pareto front that the formulation of the membership function can be presented as (12):

$$\mu_k^z = \begin{cases} \dfrac{f_k^{Max} - f_k(X^z)}{f_k^{Max} - f_k^{Min}} & f_k^{Min} \leqslant f_k(X^z) \leqslant f_k^{Max} \\[2mm] 0 & Otherwise \end{cases} \tag{12}$$

$$\forall k \in K,\ \forall z \in 0, 1, ..., q$$

The optimal values of the membership function can be calculated from (13):

$$\mu^z = \frac{\displaystyle\sum_{k \in \Omega^K} w_k \mu_k^z}{\displaystyle\sum_{k \in \Omega^K}\sum_{z \in \Omega^Z} w_k \mu_k^z}\quad \forall z \in 0, 1, ..., q \tag{13}$$

$$\sum_{k \in \Omega^K} w_k = 1$$

where w_k is the weight of the kth objective function.

The robust optimization process is utilized to solve the proposed objective function of the DA problem. The detailed formulation of robust optimization is available in [30] and is not shown for the sake of space. The real-time optimization problem is a MILP procedure that is solved by CPLEX solver.

4. Simulation results

The 70-bus test system was utilized to evaluate the suggested model. Fig. 5 presents the topology of the test system. The data of the 70-bus test system are available in [31]. The test system consists of four zones, four zonal DRAs and EVPLAs, and multiple DERs. The simulation was carried out on a PC (Intel Core i7-870 processor, 4*2.93 GHz, 8 GB RAM). The price of active power and ancillary services is available in [32]. The day-ahead and real-time price data were for March 18, 2020. Numerous scenarios were generated and reduced for wind turbine and photovoltaic electricity generation, EVPLAs and DRAs contribution scenarios, day-ahead and real-time electricity market prices, and loads [33–34]. The scenario generation and reduction parameters are presented in Table 2. The scenario generation method was applied to generate the scenario tree. A set of 1000 scenarios was generated for the solar irradiation, wind turbine power generation, EVPLAs contribution, DRAs contribution, day-ahead load and prices, and real-time load and prices. The total number of scenarios in the scenario tree was 1000^6, which led to the curse of dimensionality of the optimization problem. The scenario reduction method was utilized to reduce the scenarios to 10 each. Fig. 6 presents the forecasted day-ahead active power, reactive power, regulating reserve, and spinning reserve demand of ADS for one of the reduced scenarios.
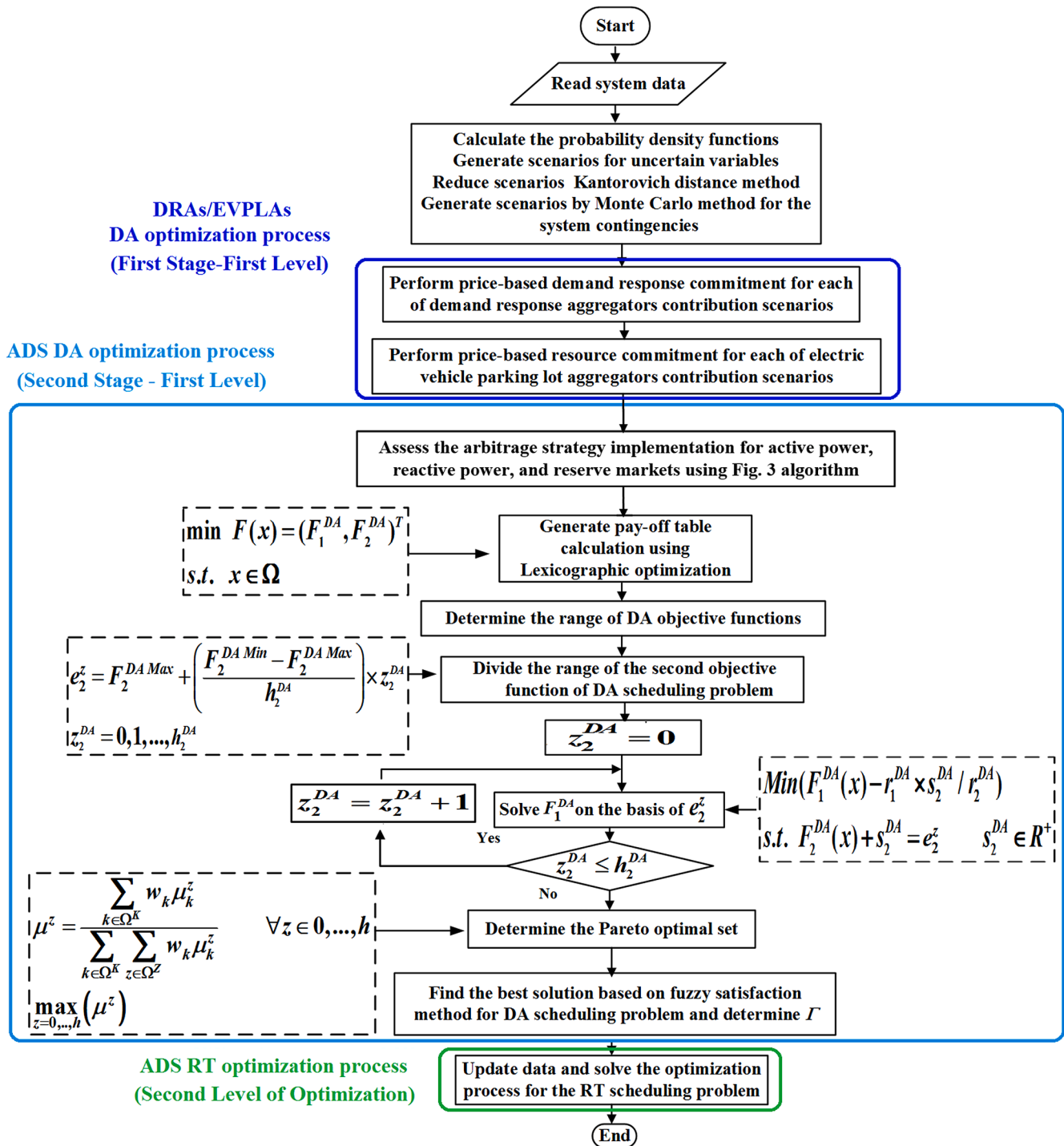
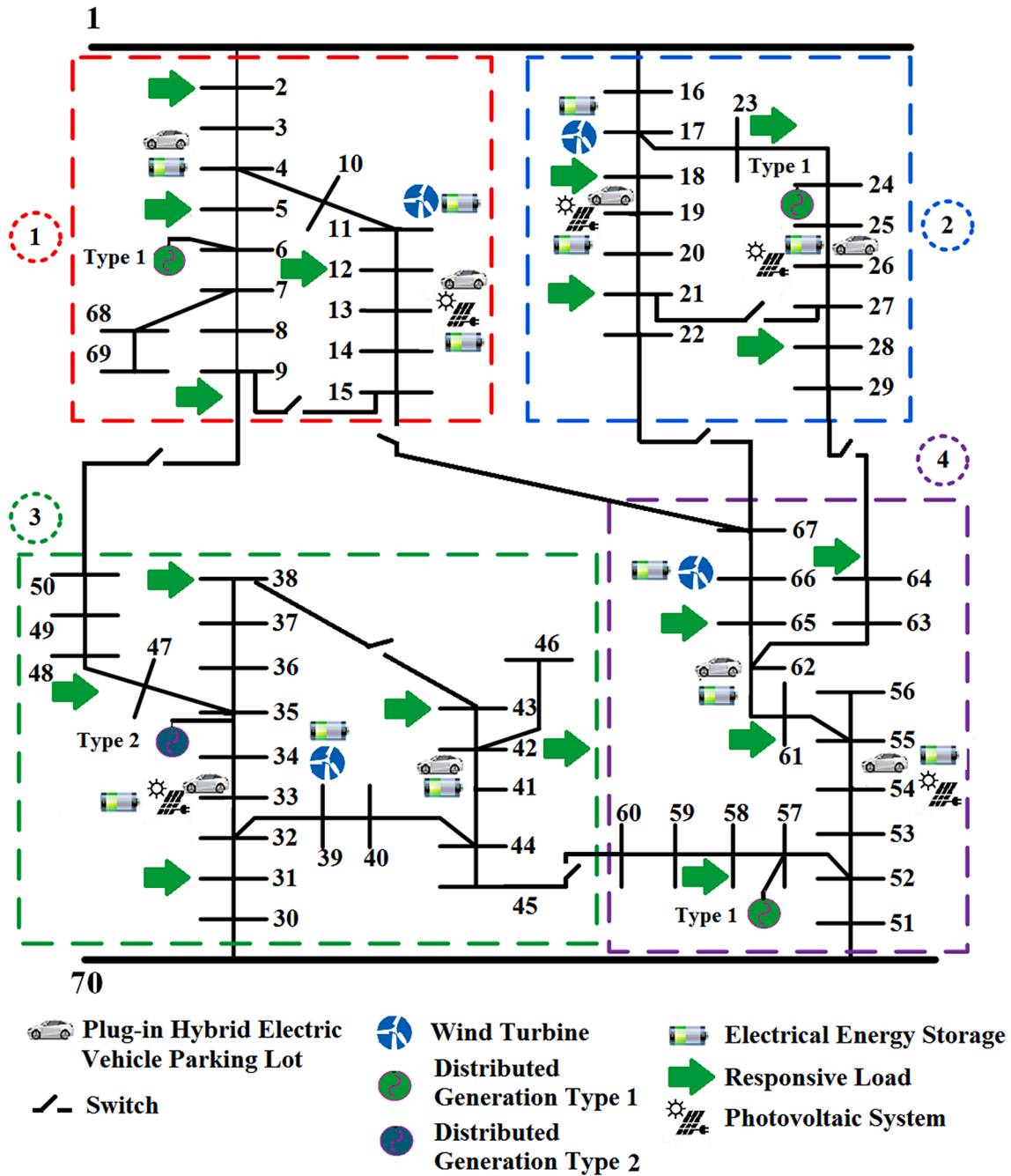**Fig. 4.** The flowchart of the day-ahead and real-time optimization process.

Fig. 5. The topology of the 70-bus test system.

Table 2
The scenario generation and reduction parameters.

System parameter	Value
Number of solar irradiation scenarios	1000
Number of wind turbine power generation scenarios	1000
Number of EVPLAs contribution scenarios	1000
Number of DRAs contribution scenarios	1000
Number of day-ahead system load and price scenarios	1000
Number of real-time system load and price scenarios	1000
Number of solar irradiation reduced scenarios	10
Number of wind turbine power generation reduced scenarios	10
Number of EVPLAs contribution reduced scenarios	10
Number of DRAs contribution reduced scenarios	10
Number of day-ahead system load and price reduced scenarios	10
Number of real-time market load and price reduced scenarios	10
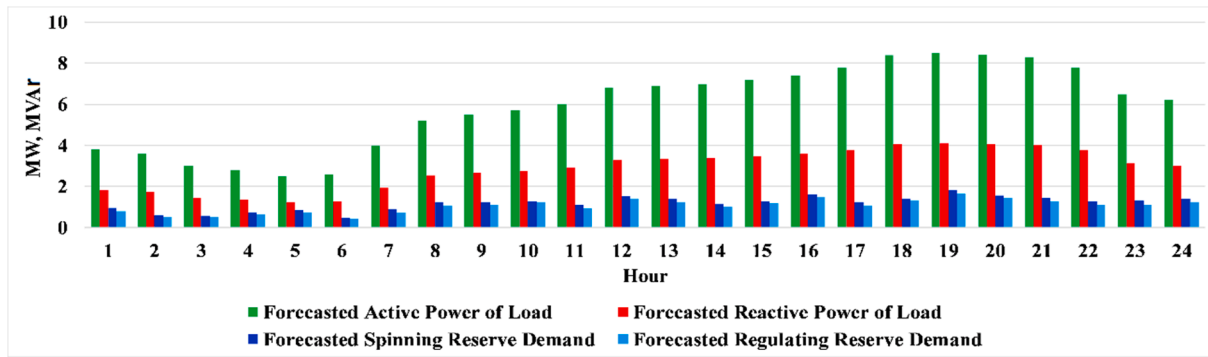
Fig. 6. The forecasted active power, reactive power, regulating reserve, and spinning reserve demand of ADS for one of the reduced scenarios.

Fig. 7 (a) depicts the forecasted day-ahead active power price for the reduced scenarios in Monetary Units (MUs). Fig. 7 (b) shows the forecasted day-ahead reactive power price for the reduced scenarios. The maximum values of active power and reactive power prices were 380 MU/kWh and 94.98 MU/kVArh, respectively. The minimum values of active power and reactive power prices were 11 MU/kWh and 1.1219 MU/kVArh, respectively. Fig. 7 (c) presents the forecasted price of active power and ancillary services in the day-ahead and real-time markets for one of the reduced scenarios.

Fig. 8 (a) depicts the perunit values of electricity generation of photovoltaic arrays for the reduced scenarios. Fig. 8 (b) shows the perunit values of electricity generation of wind turbines for the reduced scenarios.

Fig. 8 (c) presents the estimated stack column of wind and photovoltaic power generation for the DA scheduling horizon for one of the reduced scenarios. At the first stage, the PBDRC procedure for demand response aggregators and the PBRC process for plug-in hybrid electric vehicle parking lot aggregators were performed by the distribution system operator to assess the DRAs and EVPLAs contributions scenarios.

Fig. 9 (a) depicts the estimated values of the DRAs active power injection/withdrawal for the reduced scenarios. The maximum DRAs active power injection value was 726.29 kW for the fourth scenario. Further, the maximum DRAs active power injection value was 665.05 kW for the fifth scenario. Fig. 9 (b), (c) present the estimated values of the DRAs active and reactive powers for one of the reduced scenarios, respectively. As shown in Fig. 9 (b), the DRAs injected active power for 01:00–06:00 h and consumed active power for 07:00–24:00 h. The DRAs aggregated submitted bids for active and reactive energies were −4416.72 kWh and −2126.94 kVArh, respectively. The DRAs net transacted active and reactive energies were −3650.0 kWh and −1781.15 kVArh, respectively. Thus, it can be concluded that the average value of the accepted DRAs bids was about 82.64% concerning their submitted bids. Further, the maximum active and reactive power withdrawal of DRAs were 612.50 kW and 294.96 kVAr, respectively. The maximum active and reactive energy injection of DRAs were 961.81 kW and 463.17 kVAr, respectively.

Fig. 10 (a) shows the estimated values of the EVPLAs active power injection/withdrawal for the reduced scenarios. The maximum EVPLAs active power injection value was 454.42 kW for the fourth scenario. Further, the maximum EVPLAs active power injection value was 809.78 kW for the fifth scenario. Fig. 10 (b), (c) depict the estimated values of the EVPLAs active and reactive powers for one of the reduced scenarios,

respectively. The EVPLAs consumed active power for 08:00–16:00 h and injected active power for other hours of the operating horizon. The EVPLAs aggregated submitted bids for active and reactive energies were −180.69 kWh and −87.01 kVArh, respectively. The EVPLAs net transacted active and reactive energies were −3.39 kWh and −1.59 kVArh, respectively. Thus, it can be concluded that the net transacted energy of EVPLAs had a near-zero value for the 24-hour operating interval. Further, the maximum active and reactive power withdrawal of EVPLAs were 1038.15 kW and 499.85 kVAr, respectively. The maximum active and reactive energy injection of EVPLAs were 485.22 kW and 233.62 kVAr, respectively.

Fig. 11 depicts the estimated values of spinning and regulating reserves that were provided by the EVPLAs and accepted by the ADS for one of the reduced scenarios. The maximum values of spinning and regulating reserves were 602.64 kW and 552.01 kW, respectively.

Then, the distribution system operator optimized the day-ahead scheduling simulation for different values of Γ. Fig. 12 presents the aggregated active power of DRAs, EVPLAs, intermittent electricity generations, and DGs for DA scheduling. Further, the ADS active power and spinning reserve bids/offers for Γ = 0 are presented in Fig. 12. As shown in Fig. 7 (c), for multiple hours, the price of the spinning reserve was greater than that of the energy market. Thus, an arbitrage between energy and spinning reserve was carried out by the ADS operator. The ADS operator utilized the arbitrage strategy for active power, reactive power, and reserve markets when the energy and ancillary services prices were different in the scheduling horizon. The ADS operator purchased the energy and ancillary services when their prices were low and sold them when their prices were high. The maximum and minimum values of the active power of ADS offer and bid were 6074.63 kW and 1168.68 kW, respectively. The maximum and minimum values of the spinning reserve of ADS offer were 4724.3 kW and 359.82 kW, respectively.

Fig. 13 depicts the aggregated reactive power of DRAs, EVPLAs, intermittent electricity generations, and DGs for DA scheduling. Further, the ADS reactive power bids/offers for Γ = 0 are presented in Fig. 13. The maximum and minimum values of reactive power of ADS offer and bid were 2940.73 kVAr and 565.79 kVAr, respectively.
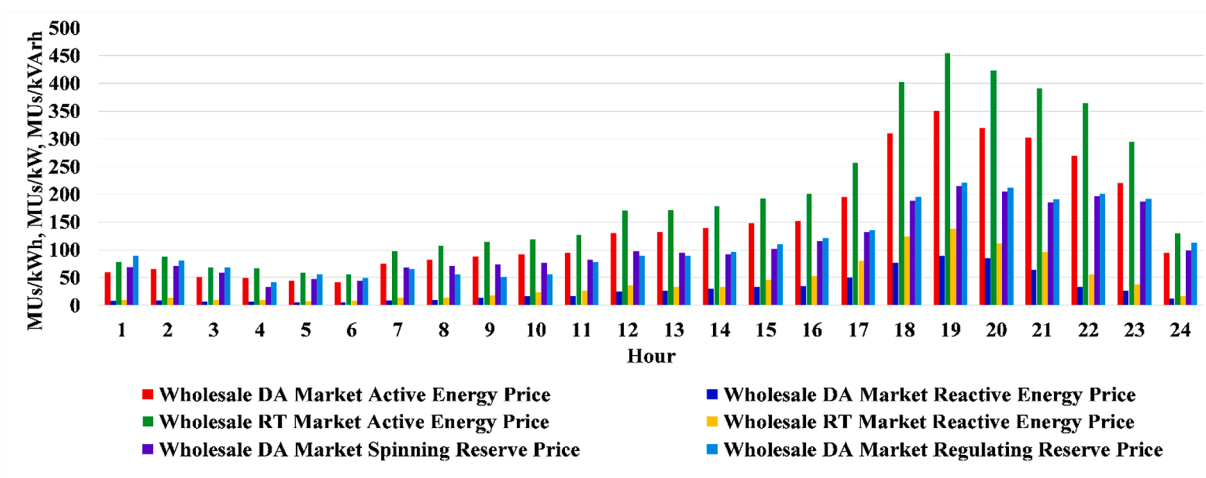
Fig. 14 presents the active power generation of ADS DERs, active and reactive power transactions of ADS with the wholesale market for Γ = 0 and Γ = 24, respectively. The ADS generated 206,097 kWh and 210,501 kWh active energy for Γ = 0 and Γ = 24, respectively. Further, the ADS transacted active energy with the wholesale market were
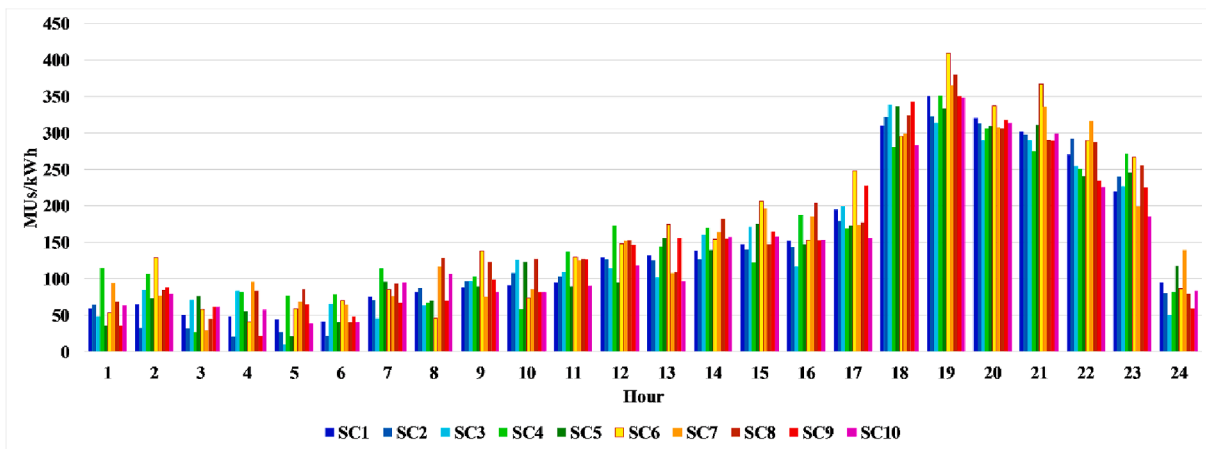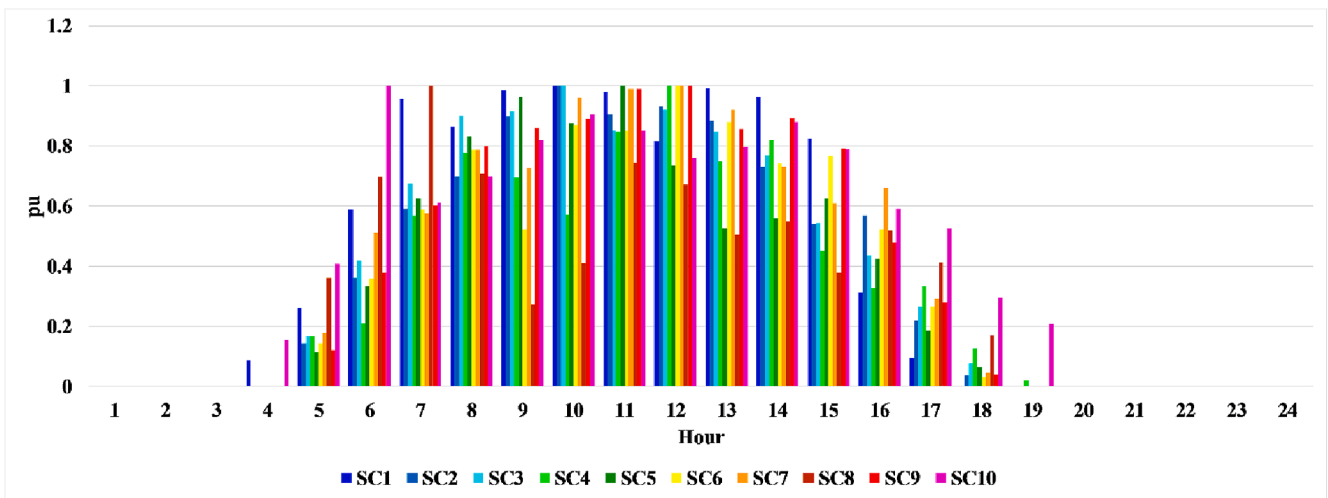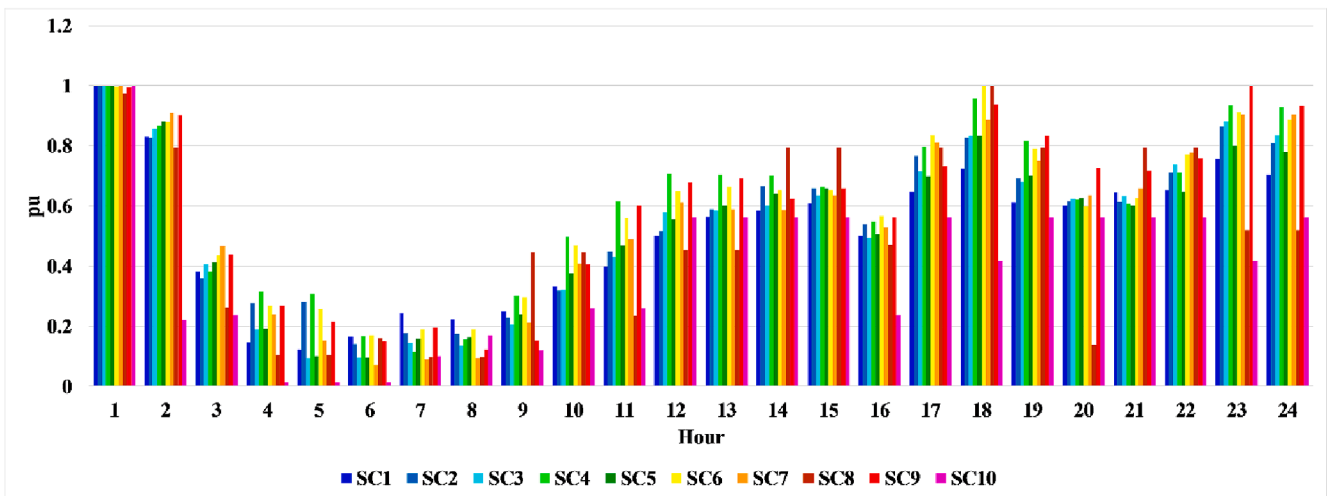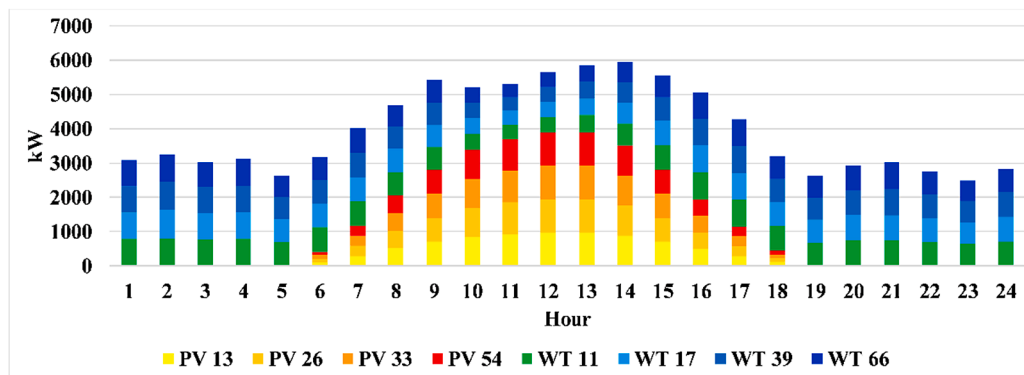
(a)
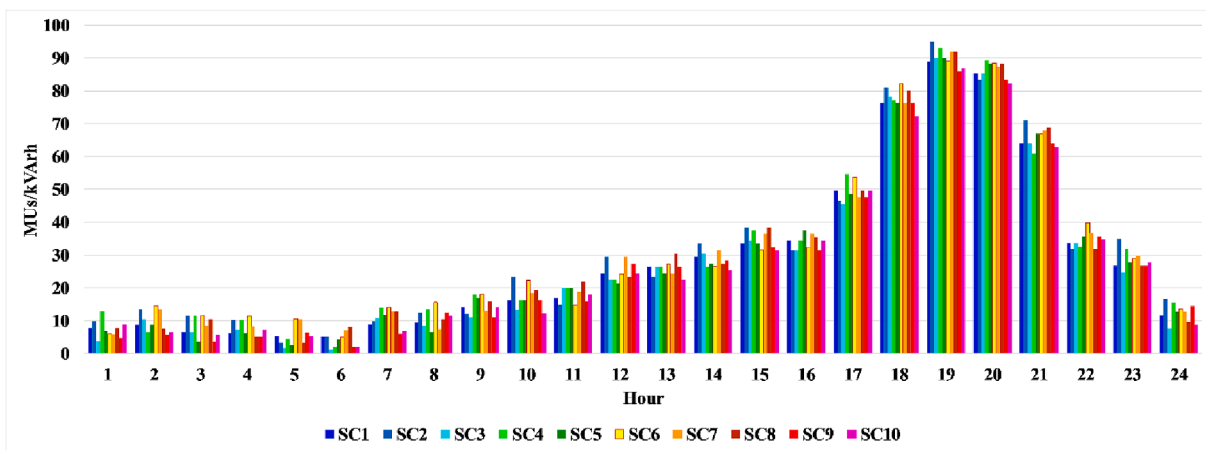
(b)

(c)

Fig. 7. (a). The forecasted day-ahead active power price for the reduced scenarios. (b) The forecasted day-ahead active power price for the reduced scenarios. (c) The forecasted price of active power and ancillary services in the day-ahead and real-time markets for one of the reduced scenarios.
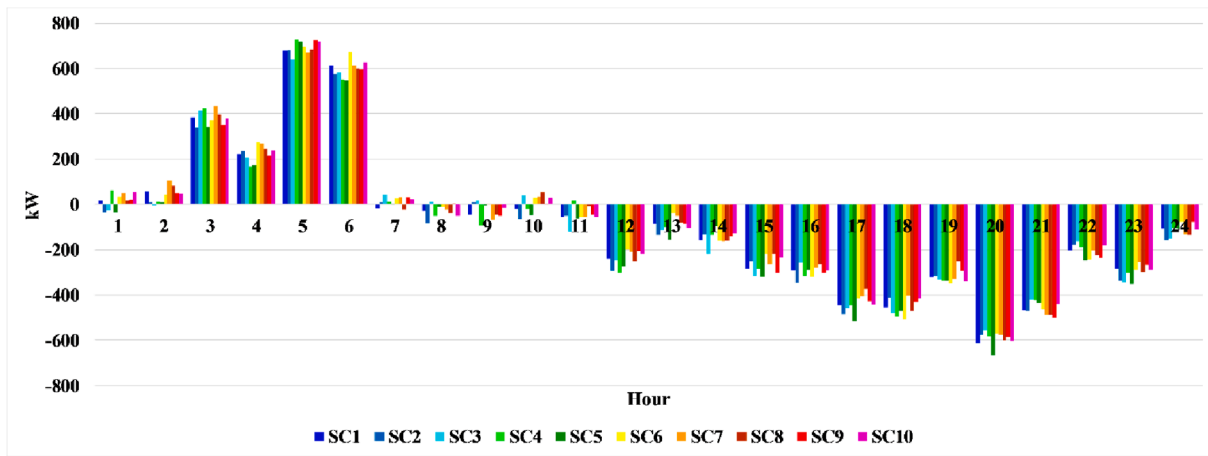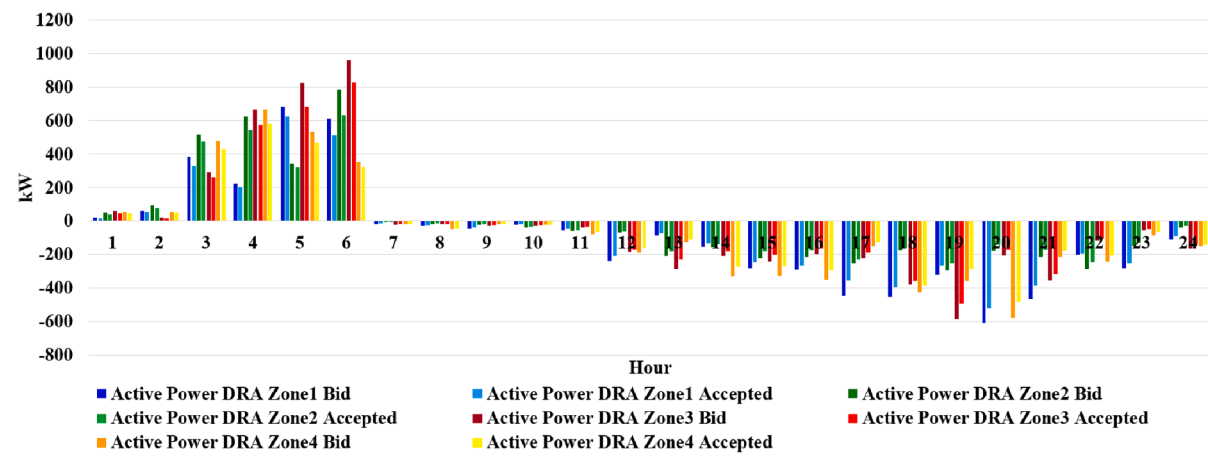
(a)

(b)

(c)

Fig. 8. (a). The perunit values of electricity generation of photovoltaic arrays for the reduced scenarios, Fig. 7 (b). The perunit values of electricity generation of wind turbines for the reduced scenarios, Fig. 7 (c). The estimated stack column of DA intermittent power generations for one of the reduced scenarios.
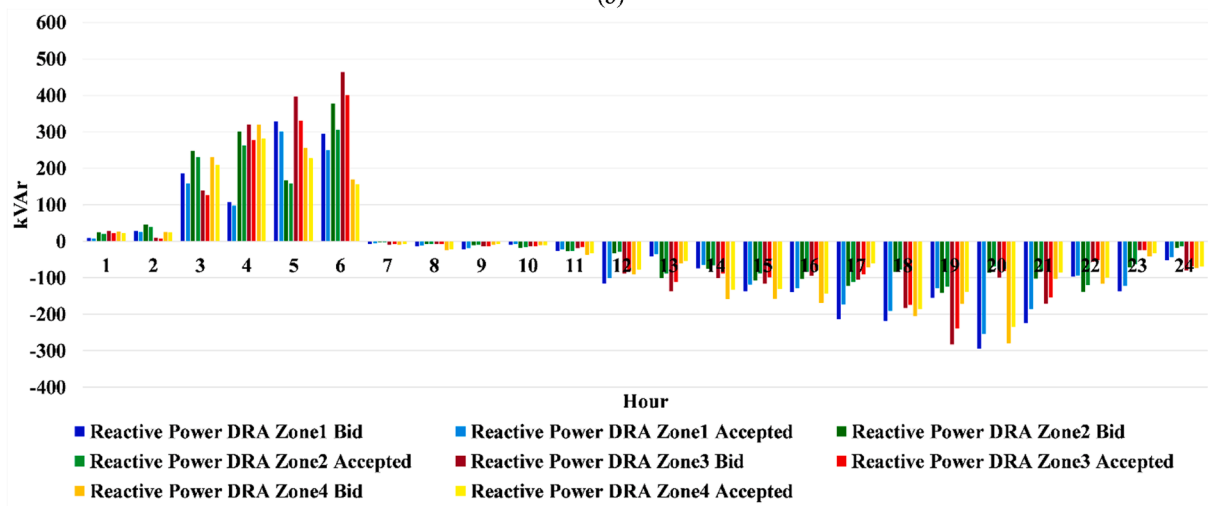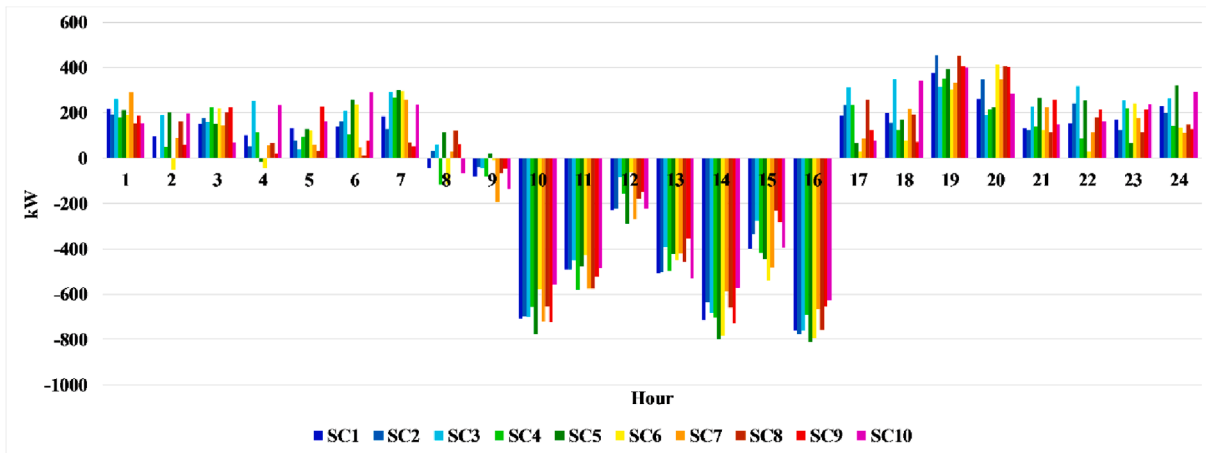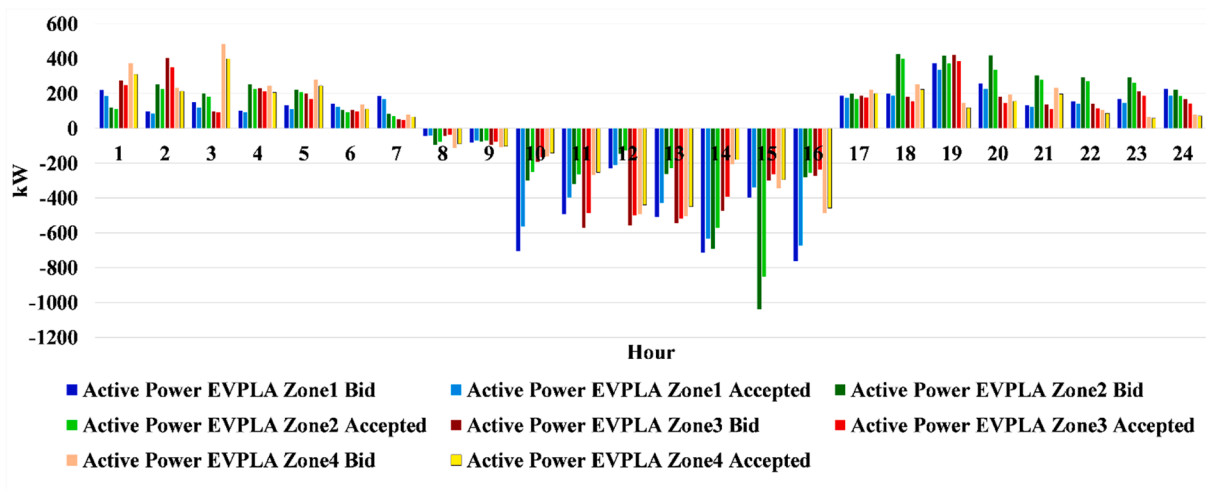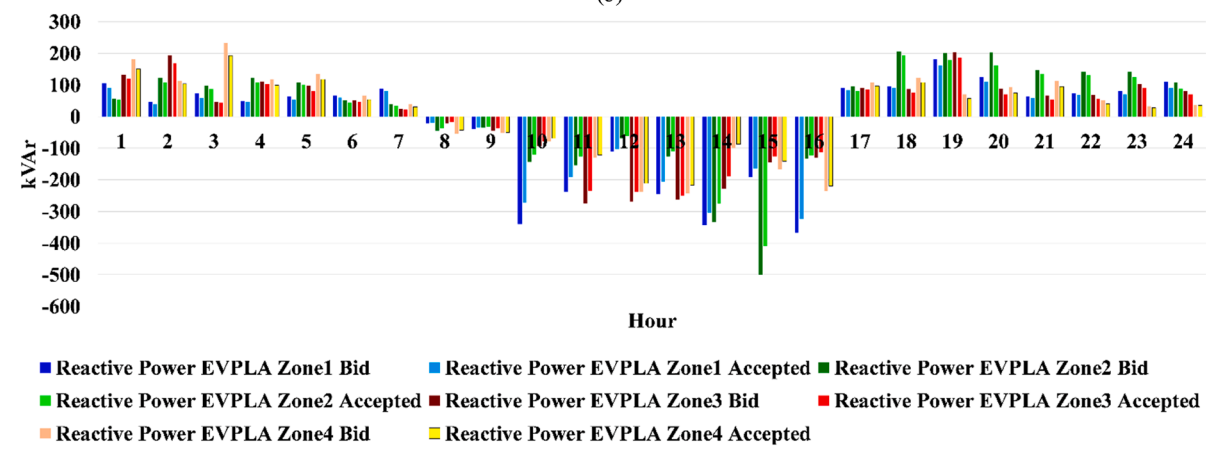
(a)

(b)

(c)

Fig. 9. (a) The estimated values of the DRAs active power injection/withdrawal for the reduced scenarios, (b) The estimated values of submitted values of DRAs active power bids and accepted values of DRAs active power bids for one of the reduced scenarios, (c) The estimated values of submitted values of DRAs reactive power bids and accepted values of DRAs active power bids for one of the reduced scenarios.

(a)

(b)

(c)

Fig. 10. (a) The estimated values of the EVPLAs active power injection/withdrawal for the reduced scenarios, (b) The estimated values of submitted values of EVPLAs active power bids and accepted values of EVPLAs active power bids for one of the reduced scenarios, (c) The estimated values of submitted values of EVPLAs reactive power bids and accepted values of EVPLAs active power bids for one of the reduced scenarios.
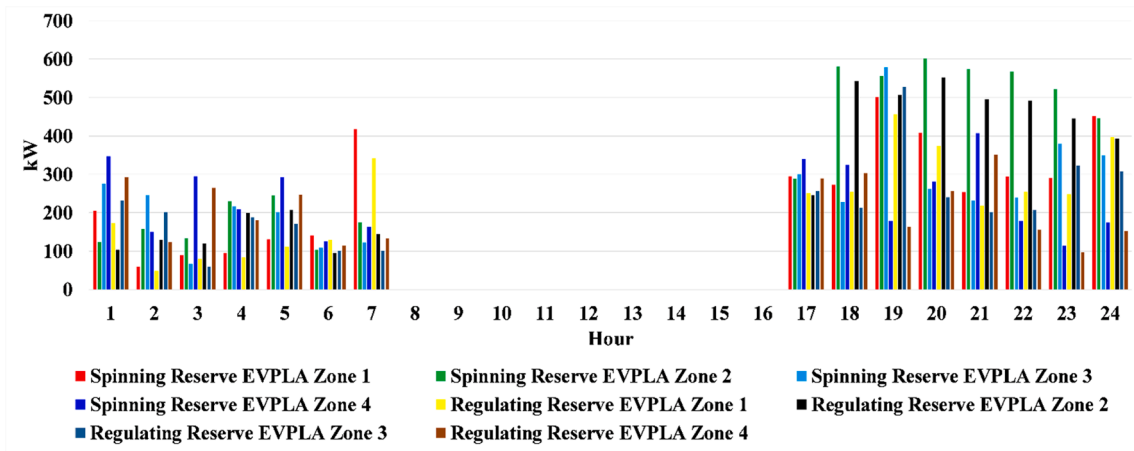
Fig. 11. The estimated values of accepted bids of EVPLAs spinning and regulating reserves for one of the reduced scenarios.
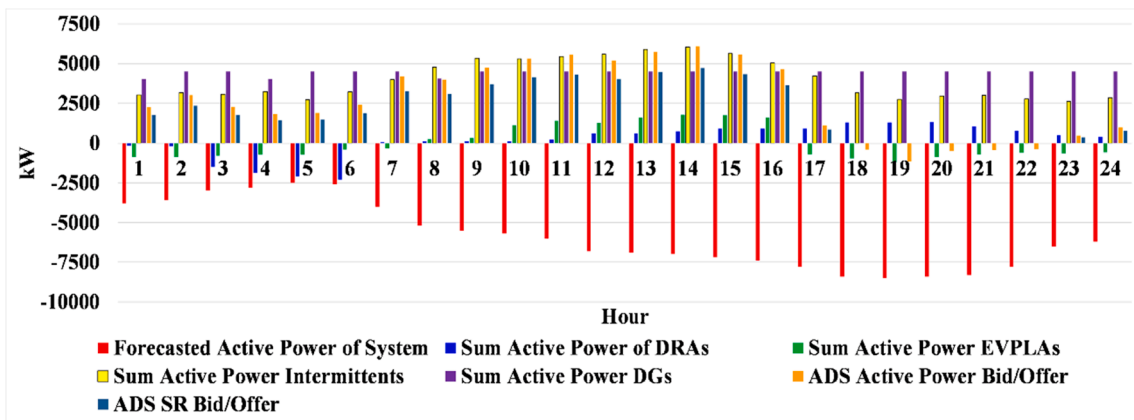

Fig. 12. The active power of DRAs, EVPLAs, ADS DERs, and ADS active power and spinning reserve bid/offer for DA scheduling and Γ = 0.
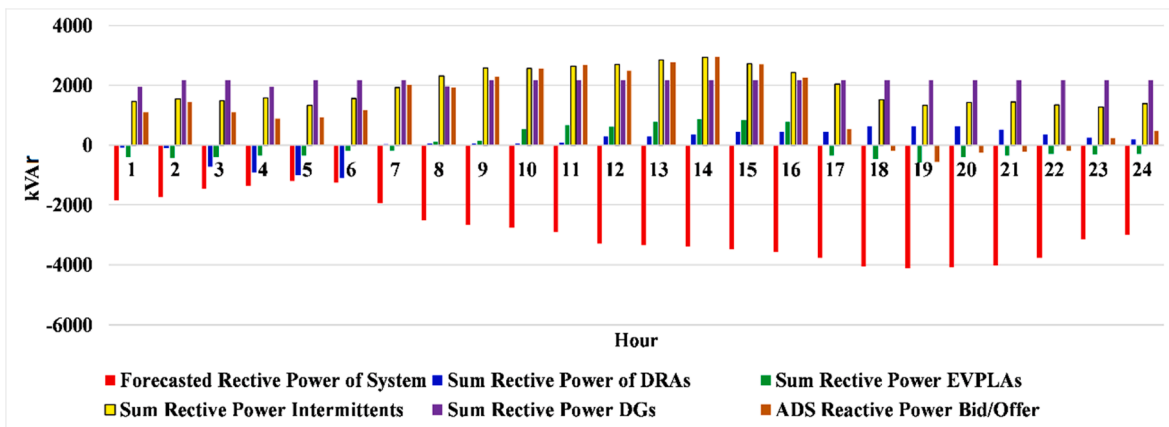

Fig. 13. The reactive power of DRAs, EVPLAs, ADS DERs, and ADS reactive power bid/offer for DA scheduling and Γ = 0.
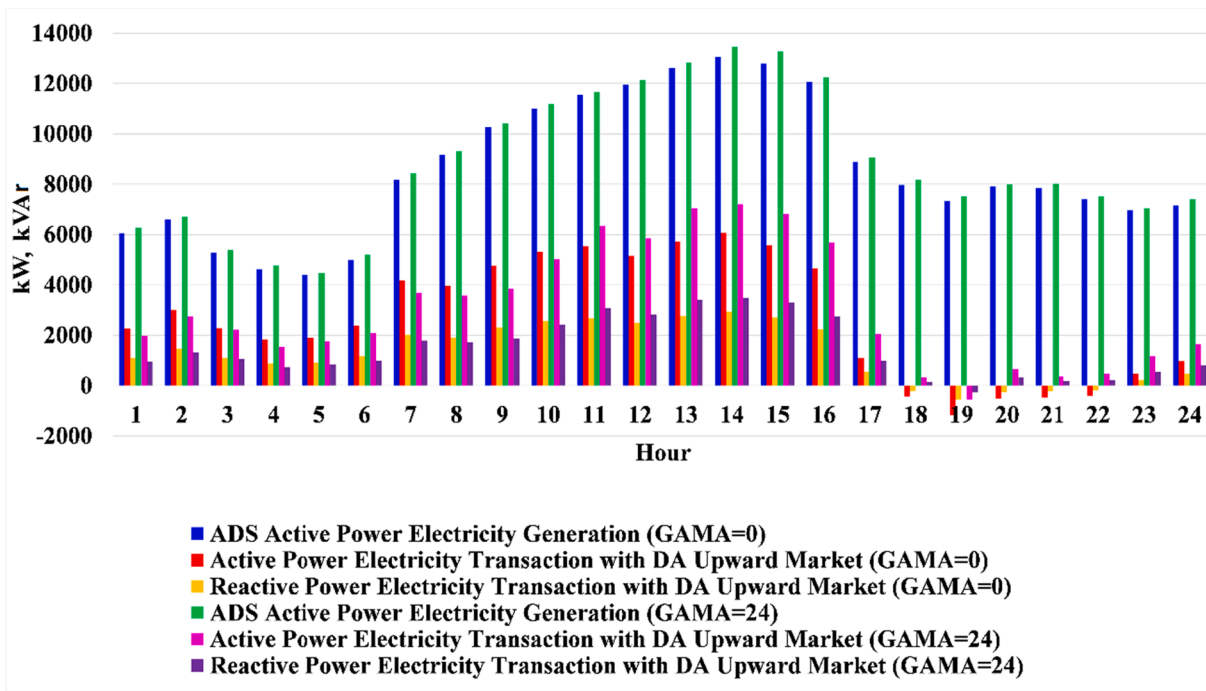
Fig. 14. The active power generation of ADS DERs, active and reactive power transaction of ADS with the wholesale market for $\Gamma = 0$ and $\Gamma = 24$.

64196.6 kWh and 73483.3 kWh for $\Gamma = 0$ and $\Gamma = 24$, respectively. The ADS produced more active power for $\Gamma = 24$ by about 2.13% concerning the $\Gamma = 0$ case based on the fact that the ADS adopted the risk-averse strategy. Further, the ADS delivered more electrical energy to the wholesale market for $\Gamma = 24$ by about 14.46% concerning the $\Gamma = 0$ case.

The 70–bus system has 68 lines, and eight normally opened switches. Thus, the total number of N-1 contingency was $68 + 70 = 138$. The contingencies of the line (1–2), (1–16), (51–70), (30–70) were not considered in the contingency ranking analysis based on the fact that the described contingencies did not lead to any load shedding process and the proposed method completely restored the system after occurring these contingencies. Thus, the second objective function for these contingencies took on a value of zero. Further, the contingencies of bus 1 and bus 70 were not considered based on the fact that these contingencies led to system blackout. Hence, the number of N-1 contingencies was 132. The proposed method considered 132*2 cascading contingencies for each hour of day-ahead optimization horizon and found the optimal scheduling of system resources and switching system switches.

Fig. 15 depicts the number of optimal switching of tie-switches for the 1–264 contingencies that were considered in the day-ahead optimization process. As shown in Fig. 15, the maximum and the minimum number of system switching were six and three, respectively. The day-ahead optimization problem maximized the objective function in contingent conditions and optimally dispatched the distribution system resources, DRAs, and EVPLAs. The average number of switching was about 4.991 for the day-ahead problem. Further, the total number of switching was 28468.

Finally, the distribution system operator optimized the real-time scheduling simulation. Fig. 16 shows the estimated values of active and reactive power transactions of ADS with the wholesale market for the real-time optimization stage and $\Gamma = 0$ and $\Gamma = 24$, respectively.

Further, Fig. 16 presents the values of active and reactive power transactions of ADS with the wholesale market for the real-time optimization stage. The estimated values of the transacted active energy of ADS in the real-time market that were calculated in the first stage problem were 19929.8 kWh and 8780.3 kWh for $\Gamma = 0$ and $\Gamma = 24$, respectively. Further, the corresponding values of reactive energy were 9648 kVArh and 4250.6 kVArh for $\Gamma = 0$ and $\Gamma = 24$, respectively. However, the estimated values of transacted active and reactive energy of ADS that were calculated in the second stage problem for the real-time market were 13189.4 kWh and 6384.9 kVArh, respectively.

Fig. 17 presents the optimal values of the first and second objective functions of the first stage optimization problem for different values of Γ and 264 contingency scenarios. As shown in Fig. 17, the optimization process determined the optimal values of Γ for the system contingencies. The optimal values of the first objective function of the day-ahead problem were highly decreased, and the optimization process selected the higher values of Γ based on the fact that the ADS imported more energy from the wholesale market in the worst-case contingencies. The values of the first and second objective functions and the selected Γ for the worst-case contingency were -16369 MUs, 88,720 MUs, and 24, respectively. The maximum value of the first objective function was 27,490 MUs and the corresponding value of the second objective function was 246,178 MUs. The real-time problem explored the total available and optimal switching of zonal switches for minimizing the *CICs* values. The total number of switching of zonal switches for the real-time process was 408,038 for the entire scheduling horizon.

For assessing the effectiveness of the proposed algorithm, the following cases were considered:

(1) Proposed algorithm without switching of zones switches,
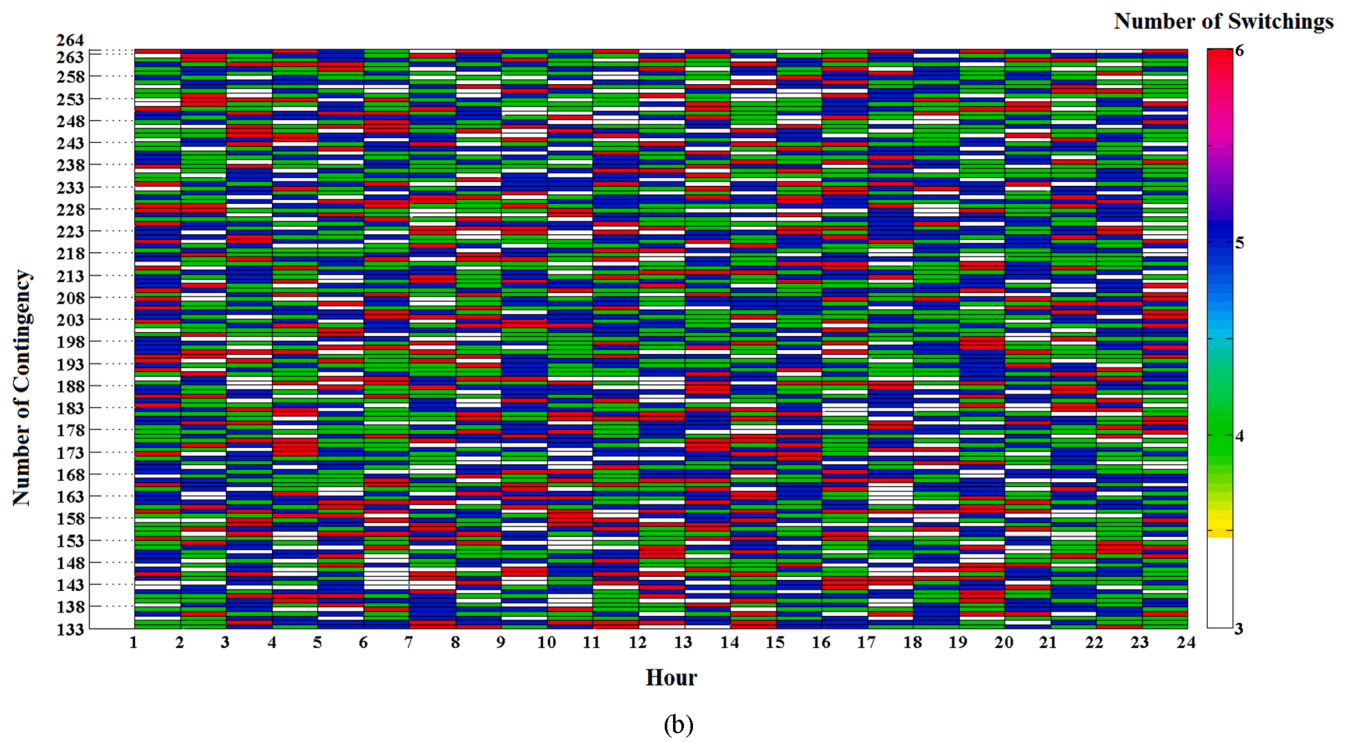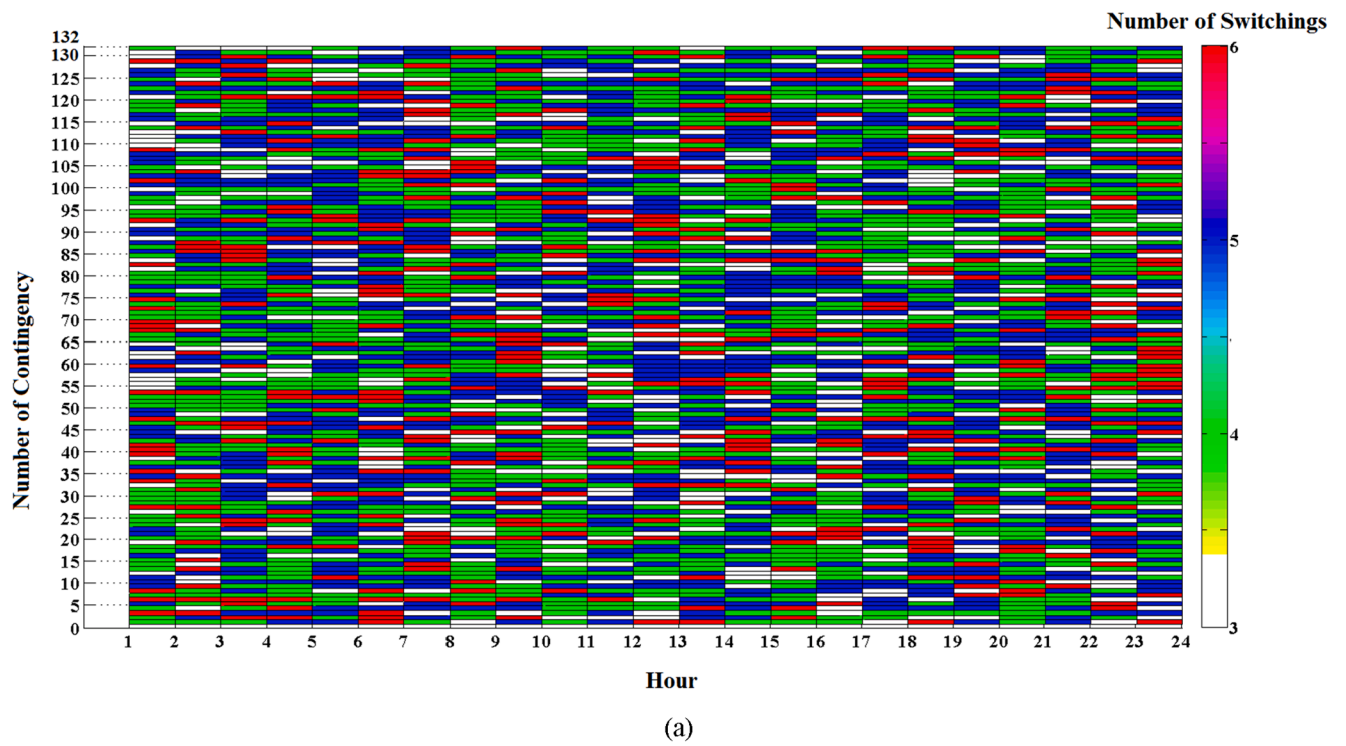(2) Proposed algorithm without ADS arbitrage,

(a)

(b)

Fig. 15. (a). The number of optimal switching of tie-switches for the 1–132 contingencies for the day-ahead optimization process, (b). The number of optimal switching of tie-switches for the 133–264 contingencies for the day-ahead optimization process.
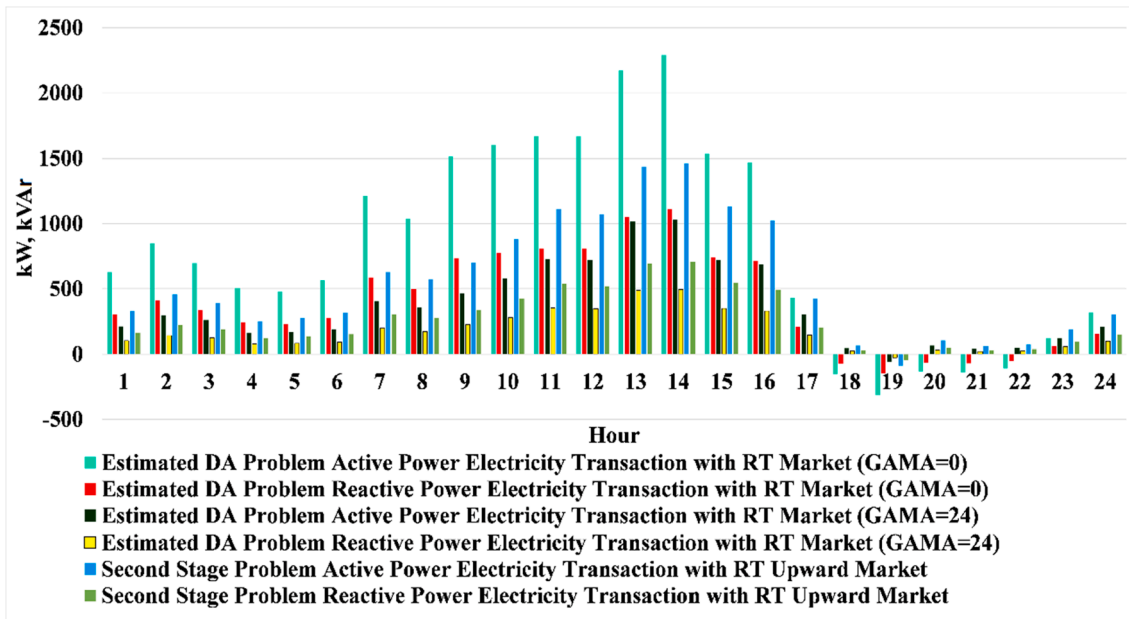
Fig. 16. The estimated values of active and reactive power transactions of ADS with the real-time wholesale market.
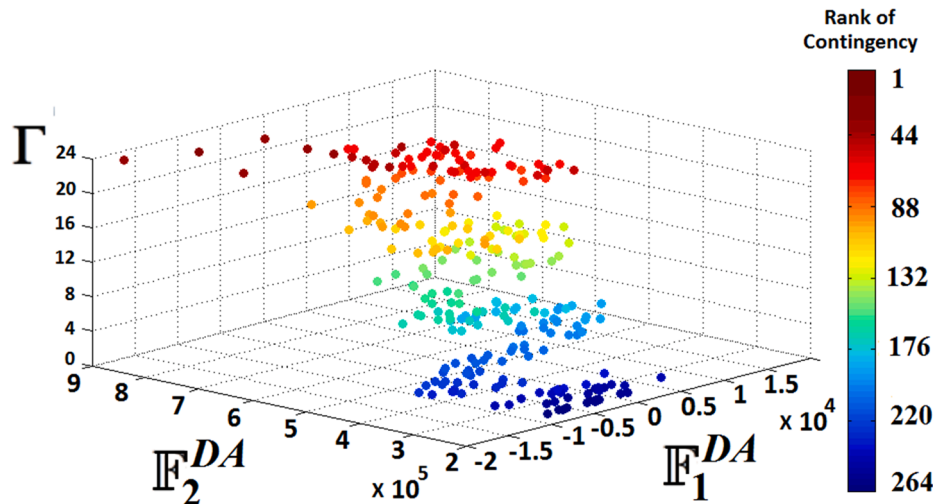

Fig. 17. The optimal values of the first and second objective functions of the first stage optimization problem for different values of Γ and contingency scenarios.

Table 3
The objective functions of the day-ahead and real-time optimization problem for the defined cases.

Average Value	Proposed Algorithm	Case 1	Case 2	Case 3	Case 4
$\mathbb{F}_1^{DA}$ (MUs)	8917.36	3279.29	5863.25	10397.42	12369.41
$\mathbb{F}_2^{DA}$ (MUs)	506620.17	1692057.2	512392.12	486367.29	469216.36
$\mathbb{S}^{RT}$ (MUs)	7749.22	−2591.36	5269.98	8969.74	9189.61

(3) Proposed algorithm without EVPLAs arbitrage,
(4) Proposed algorithm without DRAs arbitrage.

Table 3 presents the average value of the objective functions of the day-ahead and real-time optimization problem for the defined cases.

As shown in Table 3, the $\mathbb{F}_1^{DA}$, $\mathbb{F}_2^{DA}$ and $\mathbb{S}^{RT}$ changes for the first case were −63.23%, 233.99%, and −133.44% concerning the corresponding values of the proposed algorithm, respectively. The proposed algorithm

utilized the switching process to redispatch the system resources and reduce the ENSC in the real-time horizon. It can be concluded that the switching procedure highly increased the profit of the system; meanwhile, this process reduced the expected energy not supplied costs. The day-ahead and real-time revenues of ADS were reduced based on the fact that the ADS imports more electricity from the wholesale market in contingency conditions. For the second case study, the $\mathbb{F}_1^{DA}$, $\mathbb{F}_2^{DA}$ and $\mathbb{S}^{RT}$ changes were −34.25%, 1.14%, and −31.98% concerning the
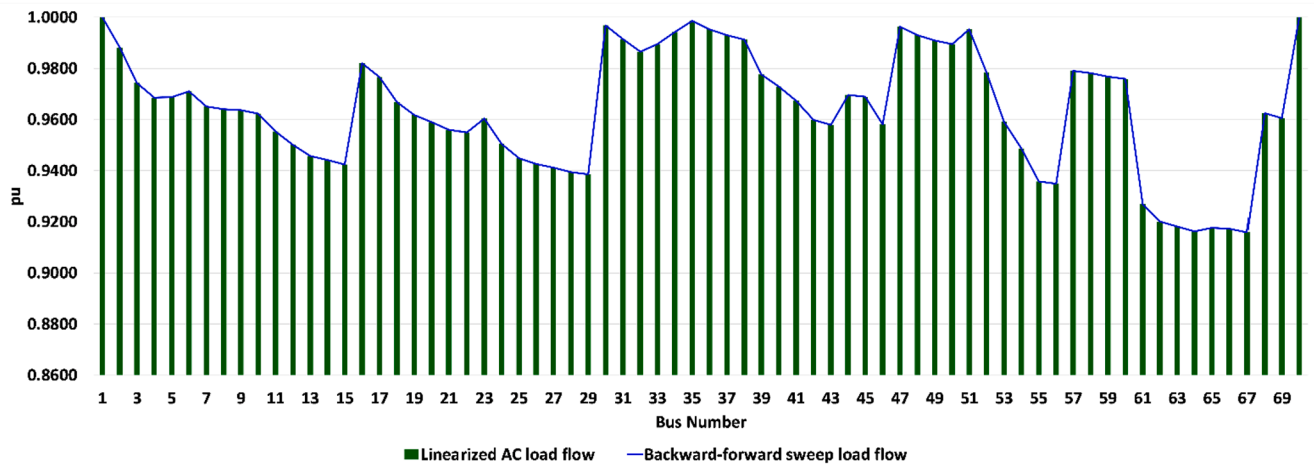
Fig. 18. The voltage magnitudes of the 70-bus test system was calculated by the backward-forward sweep load flow and linearized AC load flow.

Table 4
The objective functions of the day-ahead and real-time optimization problem for the linear and non-linear models.

Average Value	Proposed Linear Algorithm	Non-linear Model
$\mathbb{F}_1^{DA}$ (MUs)	8917.36	8793.29
$\mathbb{F}_2^{DA}$ (MUs)	506620.17	536981.25
$\mathbb{S}^{RT}$ (MUs)	7749.22	7493.17

corresponding values of the proposed algorithm, respectively. As shown in Table 3, when the ADS did not adopt the arbitrage strategy, the ADS day-ahead and real-time revenues were reduced, and the ENSC was increased. In the second case, the ENSC term was increased because the ADS load was higher than the case without the proposed method in contingency conditions. Thus, it can be concluded that the proposed algorithm increased the day-ahead and real-time revenues of the system by about 52.09% and 47.04% concerning values without the proposed method, respectively.

The $\mathbb{F}_1^{DA}$, $\mathbb{F}_2^{DA}$ and $\mathbb{S}^{RT}$ changes for the third case were 16.6%, −4.12%, and 15.75%, respectively. Further, the $\mathbb{F}_1^{DA}$, $\mathbb{F}_2^{DA}$ and $\mathbb{S}^{RT}$ changes for the fourth case were 38.71%, −7.38%, and 18.59%, respectively. For the third and fourth cases, without the arbitrage strategy of EVPLAs and DRAs, the revenues of ADS in day-ahead and real-time horizons were increased; meanwhile, the ENSC was decreased because the arbitrage strategy of aggregators reduced the availability of cheaper energy resources in normal and contingent conditions.

The linearized AC load flow constraints were considered in the proposed optimization model [26]. As presented in [26], the error of the linearization method can be calculated as (14):

$$\varepsilon = [1/cos(\pi/2^{\zeta+1})] -1 \quad (14)$$

where ζ is a parameter that determines the number of additional constraints and variables that should be added to the problem in order to linearize the AC load flow equations [26]. It was assumed: $\zeta = 13$. Thus, the error of the linearization method was $\varepsilon = 7.353428$ E-8. For assessing the linearized AC load flow accuracy, the

outputs of backward-forward sweep load flow were compared with the outputs of linearized AC load flow. Fig. 18 presents the voltage magnitudes of the 70-bus test system calculated by the backward-forward sweep load flow and linearized AC load flow. As shown in Fig. 18, the outputs of linearized AC load flow advocated the linear method's high accuracy. Using the linearized AC load flow, the maximum CPU time required to solve the proposed day-ahead optimization problem was less than 512 s. Further, for assessing the linear optimization model, a comparison was made between the outputs of the proposed linear optimization process and the non-linear optimization procedure. The non-linear model considered the non-linearity of Eq. (7), Eq. (8), and the optimization problem constraints. The DICOPT solver of GAMS solved the non-linear problems [24]. The maximum CPU time required to solve the non-linear day-ahead optimization problem was less than 3795 s using the DICOPT solver.

Table 4 presents the average value of the objective functions of the day-ahead and real-time optimization problem for the linear and non-linear models. The proposed linear optimization algorithm found the optimal solution of the problem with an acceptable computation burden.

A sensitivity analysis was accomplished to assess the effect of changing the prices of energy and ancillary services on the optimization process outputs. Table 5 shows the change in the input parameters of the optimization procedure. A single parameter sensitivity analysis is not possible to be made because the day-ahead and real-time markets prices

Table 6
The objective functions of the problem for different sensitivity analysis conditions.

		Sensitivity analysis number			
		SA0	SA1	SA2	SA3
Objective Functions	$\mathbb{F}_1^{DA}$ (MUs)	8917.36	9721.48	8382.31	10011.65
	$\mathbb{F}_2^{DA}$ (MUs)	506620.17	521818.77	486355.36	543010.40
	$\mathbb{S}^{RT}$ (MUs)	7749.22	7857.71	7516.74	8144.08

Table 5
The change in the input parameters of the optimization process.

Sensitivity Analysis	Day-ahead active power price	Day-ahead spinning reserve price	Day-ahead regulating reserve price	Day-ahead reactive power price	Real-time active-power price	Real-time reactive power price
SA0	–	–	–	–	–	–
SA1	+5%	+2%	+2%	+1%	+1%	+1%
SA2	−5%	−2%	−2%	−1%	−1%	−1%
SA3	+10%	+8%	+5%	+2%	+2%	+2%

Table 7

The scenario generation and reduction parameters.

System parameter	Value
Number of solar irradiation scenarios	1500
Number of wind turbine power generation scenarios	1500
Number of EVPLAs contribution scenarios	1500
Number of DRAs contribution scenarios	1500
Number of day-ahead market load and price scenarios	1500
Number of real-time market load and price scenarios	1500
Number of solar irradiation reduced scenarios	15
Number of wind turbine power generation reduced scenarios	15
Number of EVPLAs contribution reduced scenarios	15
Number of DRAs contribution reduced scenarios	15
Number of day-ahead market load and price reduced scenarios	15
Number of real-time market load and price reduced scenarios	15

have correlations.

Table 6 depicts the average value of the objective functions of the day-ahead and real-time optimization problem for the sensitivity analysis conditions. The changes of the first objective function of the day-ahead optimization problem ($\mathbb{F}_1^{DA}$) was about $+$ 9.01%, -6.09%, and $+$ 12.27% for the SA1, SA2, and SA3 conditions, respectively. Further, the changes of the second objective function of the day-ahead optimization problem ($\mathbb{F}_2^{DA}$) were about $+$ 2.99%, -4.01%, and $+7.18\%$ for the SA1, SA2, and SA3 conditions, respectively. Finally, the changes of the objective function of the real-time optimization problem ($\mathbb{S}^{RT}$) was about $+$ 1.4%, -3.0%, and $+5.02\%$ for the SA1, SA2, and SA3 conditions, respectively. Thus, the proposed algorithm increased the active distribution system revenue for the high energy and ancillary services prices. Further, the energy not supplied cost was increased when the energy and ancillary services prices were increased based on the fact that the cost of energy purchased from the wholesale market was increased.

Further, a sensitivity analysis was performed to assess the impacts of changing scenario generation and reduction parameters on the outputs. Table 7 presents the scenario generation and reduction parameters for sensitivity analysis.

Table 8 presents the average value of the objective functions of the day-ahead and real-time optimization problem for the defined cases and the different cases of scenario generation and reduction parameters.

As shown in Table 8, the $\mathbb{F}_1^{DA}$, $\mathbb{F}_2^{DA}$ and $\mathbb{S}^{RT}$ changes for the proposed algorithm and Table 7 parameters were 3.61%, 1.4%, and 4.9% concerning the corresponding values of Table 2 parameters, respectively. The value of $\mathbb{F}_1^{DA}$ and $\mathbb{S}^{RT}$ for different cases of Table 7 parameters were increased based on the fact that the control variables of the ADS were increased when more EVPLAs and DRAs contribution scenarios and intermittent power generation scenarios were considered in day-ahead and real-time markets. Further, the values of $\mathbb{F}_2^{DA}$ for different cases of Table 7 parameters were reduced based on the fact that the control variables of the ADS were increased when more contribution scenarios

of distributed energy resources were considered.

The proposed algorithm successfully encountered the DRAs and EVPLAs contribution scenarios and their arbitrage strategies in the day-ahead and real-time scheduling of ADS. Further, the adoption of the arbitrage strategy of the active distribution system and the optimal switching of zonal switches was carried out to optimize the objective functions.

The active distribution system operator that transacts active power and ancillary services with the wholesale market, demand response aggregators, and electric vehicle parking lot aggregators can utilize the proposed approach to maximize his/her profit. For example, an industrial electrical distribution system with a high value of distributed generation penetration factor may have more control variables to reduce the impacts of external shocks and system contingencies.

5. Conclusion

This paper introduced a novel approach to consider the arbitrage strategies of the active distribution system, and the optimal bidding strategies of plug-in hybrid electric vehicle parking lot and demand response aggregators in electricity markets. Also, the distribution system transacted energy and ancillary services with the wholesale electricity market and performed an arbitrage strategy to maximize the system benefits. The algorithm determined the optimal values of system resource commitment, robustness parameter, the status of zonal tie-line switches, and distributed energy resource aggregators' contributions. The robust and lexicographic ordering optimization methods were utilized to optimize the formulated problem. The system contingencies were assessed in the framework, and the revenues and energy not-supplied costs of the system were optimized using non-dominated solutions. The proposed algorithm increased the revenue of the active distribution system in the day-ahead and real-time horizons by about 52.09% and 47.04%, respectively, concerning the case without the proposed method. The utilization of more demand response procedures

Table 8

The objective functions of the day-ahead and real-time optimization problem for the defined cases.

Average Value	Based on Table 2 scenario generation and reduction parameters					Based on Table 7 scenario generation and reduction parameters				
	Proposed Algorithm	Case 1	Case 2	Case 3	Case 4	Proposed Algorithm	Case 1	Case 2	Case 3	Case 4
$\mathbb{F}_1^{DA}$ (MUs)	8917.36	3279.29	5863.25	10397.42	12369.41	9239.25	3369.85	6098.96	10821.3	13425.12
$\mathbb{F}_2^{DA}$ (MUs)	506620.17	1692057.2	512392.12	486367.29	469216.36	513691.2	1676941.31	494231.62	469341.12	429312.4
$\mathbb{S}^{RT}$ (MUs)	7749.22	-2591.36	5269.98	8969.74	9189.61	8129.16	-2493.51	5593.21	9232.15	9624.14

is considered for expanding this work.

Declaration of Competing Interest

The authors declare that they have no known competing financial interests or personal relationships that could have appeared to influence the work reported in this paper.

References

[1] Ma H, Liu Z, Li M, Wang B, Si Y, Yang Y, et al. A two-stage optimal scheduling method for active distribution networks considering uncertainty risk. Energy Rep 2021;7:4633–41.

[2] Zhang J, Zhou Y, Li Z, Cai J. Three-level day-ahead optimal scheduling framework considering multi-stakeholders in active distribution networks: Up-to-down approach. Energy 2021;219:119655.

[3] Zhang J, Li Z, Wang B. Within-day rolling optimal scheduling problem for active distribution networks by multi-objective evolutionary algorithm based on decomposition integrating with thought of simulated annealing. Energy 2021;223:120027. https://doi.org/10.1016/j.energy.2021.120027.

[4] Sheng H, Wang C, Liang J. Multi-timescale active distribution network optimal scheduling considering temporal-spatial reserve coordination. Int. J. Elect. Power Energy Syst. 2021;125:106526.

[5] Li Z, Su S, Jin X, Chen H, Li Y, Zhang R. A hierarchical scheduling method of active distribution network considering flexible loads in office buildings. Int. J. Elect. Power Energy Syst. 2021;131:106768.

[6] Bostan A, Setayesh Nazar M, Shafie-khah MR, Catalo JPS. Optimal scheduling of distribution systems considering multiple downward energy hubs and demand response programs. Energy 2019;190:116349.

[7] Quijano DA, Padilha-Feltrin A. Optimal integration of distributed generation and conservation voltage reduction in active distribution networks. Int. J. Elect. Power Energy Syst. 2019;113:197–207.

[8] Salehi J, Abdolahi A. Optimal scheduling of active distribution networks with penetration of PHEV considering congestion and air pollution using DR program. Sustain Cities Soc 2019;51:101709.

[9] Zhou Y, Zhang J. Three-layer day-ahead scheduling for active distribution network by considering multiple stakeholders. Energy 2020;207:118263.

[10] Saint-Pierre A, Mancarella P. Active distribution system management: A dual-horizon scheduling framework for DSO/TSO interface under uncertainty. IEEE Trans. Smart Grid 2017;8(5):2186–97.

[11] Evangelopoulos V, Avramidis I, Georgilakis P. Flexibility services management under uncertainties for power distribution systems: Stochastic scheduling and predictive real-time dispatch. IEEE Access 2018;8:38855–71.

[12] Zhao F, Si J, Wang J. Research on optimal schedule strategy for active distribution network using particle swarm optimization combined with bacterial foraging algorithm. Int. J. Elect. Power Energy Syst. 2016;78:637–46.

[13] Sadati SMB, Moshtagh J, Shafie-khah M, Catalão JPS. Smart distribution system operational scheduling considering electric vehicle parking lot and demand response programs. Electr. Power Syst. Res. 2018;160:404–18.

[14] Tan Yi, Cao Y, Li Y, Lee KY, Jiang L, Li S. Optimal day-ahead Operation considering power quality for active distribution networks. IEEE Trans. Autom. Sci. Eng. 2017;14(2):425–36.

[15] Li P, Wu Z, Wang Y, Dou X, Hu M, Hu J. Adaptive robust optimal reactive power dispatch in unbalanced distribution networks with high penetration of distributed generation. IET Gener. Transmiss. Distrib. 2018;12(6):1382–9.

[16] Golshannavaz S, Afsharnia S, Aminifar F. Smart distribution grid: Optimal day-ahead scheduling with reconfigurable topology. IEEE Trans. Smart Grid 2014;5(5):2402–11.

[17] Deng Z, Liu M, Chen H, Lu W, Dong P. Optimal scheduling of active distribution networks with limited switching operations using mixed-integer dynamic optimization. IEEE Trans. Smart Grid 2019;10(4):4221–34.

[18] Zhu X, Han H, Gao S, Shi Q, Cui H, Zu G. A multi-stage optimization approach for active distribution network scheduling considering coordinated Electrical vehicle charging strategy. IEEE Access 2018;6:50117–30.

[19] Esmaeili S, Anvari-Moghaddam A, Jadid S, Guerrero JM. Optimal simultaneous day-ahead scheduling and hourly reconfiguration of distribution systems considering responsive loads. Int. J. Elect. Power Energy Syst. 2019;104:537–48.

[20] Bostan A, Setayesh Nazar M, Shafie-khah MR, Catalo JPS. An integrated optimization framework for combined heat and power units, distributed generation and plug-in electric vehicles. Energy 2020;202:117789.

[21] Zakernezhad H, Setayesh Nazar M, Shafie-khah MR, Catalo JPS. Optimal resilient operation of multi-carrier energy systems in electricity markets considering distributed energy resource aggregators. Appl Energy 2021;299:117271.

[22] Carrano EG, Guimaraes FG, Takahashi RHC, Neto OM, Campelo F. Electric distribution network expansion under load-evolution uncertainty using an immune system inspired algorithm. IEEE Trans. Power Syst 2007;22(2):851–61.

[23] Shahidehpour M, Yamin H, Li Z. Market Operations in Electric Power Systems: Forecasting, Scheduling, and Risk Management. John Wiley & Sons; 2002, pp. 115–160.

[24] Nezamabadi H, Setayesh Nazar M. Arbitrage strategy of virtual power plants in energy, spinning reserve and reactive power markets. IET Gener. Transmiss. Distrib. 2016;10(3):750–63.

[25] Boyle G. Renewable energy, Renewable Energy, Oxford University Press; 2004, pp. 456-470.

[26] Kavousi-Fard A, Zare A, Khodaei A. Effective Dynamic Scheduling of Reconfigurable Microgrids. IEEE Trans. Power Syst. 2018;33(5):5519–30.

[27] Wang Z, Negash A, Kirschen DS. Optimal scheduling of energy storage under forecast uncertainties. IET Gener. Transm. Distrib. 2017;11:4220–6.

[28] Gunantara N, Ai Q. A review of multi-objective optimization: Methods and its applications. Cogent Eng 2018;5(1):1502242. https://doi.org/10.1080/23311916.2018.1502242.

[29] Roman C, Rosehart W. Evenly distributed Pareto points in multi-objective optimal power flow. IEEE Trans Power Syst 2006; 21(2): pp. 1011–1012.

[30] Bertsimas D, Sim M. The Price of Robustness. Oper Res 2004;52(1):35–53.

[31] Das D. A fuzzy multiobjective approach for network reconfiguration of distribution systems. IEEE Trans. Power. Del. 2006;21(1):202–9.

[32] https://www.igmc.ir/electronic-services/power-market/reports/power-market-daily-price-report.

[33] Eichhorn A, Heitsch H, Römisch W. Stochastic optimization of electricity portfolios: Scenario tree modeling and risk management. Handbook of power systems II. Springer, Berlin, Heidelberg; 2010.

[34] Heitsch H, Römisch W. Scenario reduction algorithms in stochastic programming. Comput Optimiz Appl 2003;24:187–206.